IOP PUBLISHING NONLINEARITY

Nonlinearity **22** (2009) R1–R44 doi:10.1088/0951-7715/22/1/R01

INVITED ARTICLE

The role of self-similarity in singularities of partial differential equations*

Jens Eggers[1] **and Marco A Fontelos**[2]

[1] School of Mathematics, University of Bristol, University Walk, Bristol BS8 1TW, UK
[2] Instituto de Ciencias Matemáticas, (ICMAT, CSIC - UAM - UCM - UC3M), C/Serrano 123, 28006 Madrid, Spain

Received 11 January 2008, in final form 18 November 2008
Published 17 December 2008
Online at stacks.iop.org/Non/22/R1

Recommended by A L Bertozzi

Abstract
We survey rigorous, formal and numerical results on the formation of point-like singularities (or blow-up) for a wide range of evolution equations. We use a similarity transformation of the original equation with respect to the blow-up point, such that self-similar behaviour is mapped to the fixed point of a *dynamical system*. We point out that analysing the dynamics close to the fixed point is a useful way of characterizing the singularity, in that the dynamics frequently reduces to very few dimensions. As far as we are aware, examples from the literature either correspond to stable fixed points, low-dimensional centre-manifold dynamics, limit cycles or travelling waves. For each 'class' of singularity, we give detailed examples.

Mathematics Subject Classification: 35A20

1. Introduction

Nonlinear partial differential equations (PDEs) are distinguished by the fact that, starting from smooth initial data, they can develop a singularity in finite time [1–4][3]. Very often, such a singularity corresponds to a physical event, such as the solution (e.g. a physical flow field) changing topology, and/or the emergence of a new (singular) structure, such as a tip, cusp, sheet or jet. On the other hand, a singularity can also imply that some essential physics is missing from the equation in question, which should thus be supplemented with additional terms. (Even in the latter case, the singularity may still be indicative of a real physical event).

Consider for example the physical case shown in figure 1, which we will treat in section 4. Shown is a snapshot of one viscous fluid dripping into another fluid, close to the point where

* This paper is published as part of a collection in honour of Todd Dupont's 65th birthday.
[3] Of course, there are also many examples of nonlinear PDEs for which global existence can be established!

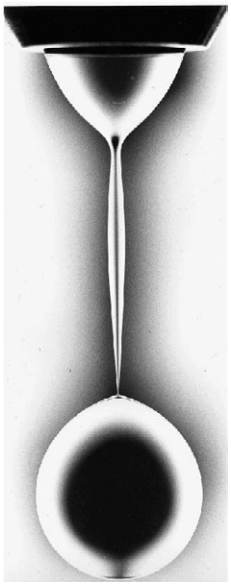

Figure 1. A drop of glycerin dripping through polydimethylsiloxane near pinch-off [5]. The nozzle diameter is 0.48 cm, the viscosity ratio is $\lambda = 0.95$. Reprinted with permission from [5]. Copyright 1999, American Institute of Physics.

a drop of the inner fluid pinches off. This process is driven by surface tension, which tries to minimize the surface area between the two fluids. At a particular point x_0, t_0 in space and time, the local radius $h(x, t)$ of the fluid neck goes to zero; this point is a singularity of the underlying equation of motion. Since the drop breaks into two pieces, there is no way the problem can be continued without generalizing the formulation to one that includes topological changes. However, in this review we adopt a broader view of what constitutes a singularity. We consider it as such whenever there is a loss of regularity, which implies that there is a length scale which goes to zero. This is the situation under which one expects self-similar behaviour, which is our guiding principle.

A fascinating aspect of the study of singularities is that they describe a great variety of phenomena which appear in the natural sciences and beyond [3]. Some examples of such singular events occur in free-surface flows [6], turbulence and Euler dynamics (singularities of vortex tubes [7, 8] and sheets [9]), elasticity [10], Bose–Einstein condensates [11], nonlinear wave physics [12], bacterial growth [13, 14], black-hole cosmology [15, 16] and financial markets [17].

In this paper we consider evolution equations

$$h_t = F[h], \tag{1.1}$$

where $F[h]$ represents some (nonlinear) differential or integral operator. We also discuss cases where h is a vector, and thus (1.1) is a system of equations. Furthermore, the spatial variable x may also have several dimensions, and thus potentially different scaling in different coordinate directions. We will cite some examples below, but few of the higher-dimensional cases have so far been analysed in detail. For the purpose of the following discussion, let us suppose that both x and h are scalar quantities, and that the singularity occurs at a single point in space and time x_0, t_0. If $t' = t_0 - t$ and $x' = x - x_0$, we are looking for local solutions of (1.1) which

have the structure

$$h(x,t) = t'^{\alpha} H(x'/t'^{\beta}), \tag{1.2}$$

with appropriately chosen values of the exponents α, β. Note that later the prime is also used to indicate a derivative. However, this will always be with respect to a spatial variable like x, z or the similarity variable ξ, hence confusion should not arise.

Giga and Kohn [18, 19] proposed to introduce self-similar variables $\tau = -\ln(t')$ and $\xi = x'/t'^{\beta}$ to study the asymptotics of blow up. Namely, putting

$$h(x,t) = t'^{\alpha} H(\xi,\tau), \tag{1.3}$$

(1.1) is turned into the 'dynamical system'

$$H_\tau = G[H] \equiv \alpha H - \beta\xi H_\xi + F[H]. \tag{1.4}$$

By virtue of (1.4), solutions to the original PDE (1.1) for given initial data can be viewed as orbits in some infinite dimensional phase, for instance, L^2. To understand the blow-up of (1.1), Giga and Kohn proposed to study the long-time behaviour of the *dynamical system* (1.4). Thus in particular, one is interested in the attractors of (1.4) (ω-limit sets in the notation which is customary in the context of PDEs, see [20] and references therein). If (1.2) is indeed a solution of (1.1), the right-hand side of (1.4) is *independent* of τ, and self-similar solutions of the form (1.2) are *fixed points* of (1.4), which we will denote by $\overline{H}(\xi)$. By studying the dynamics close to the fixed point, we find that the dynamical system (1.4) frequently reduces to very few dimensions. Thus on the one hand one obtains detailed information on the behaviour of the original problem (1.1) near blowup. On the other hand, one also gains a fruitful means of *classifying* or at least *characterizing* singularities.

The most basic linear stability analysis of this self-similar solution consists of linearizing around the fixed point according to

$$H = \overline{H}(\xi) + \epsilon P(\xi,\tau), \tag{1.5}$$

which gives

$$P_\tau = \mathcal{L}P, \tag{1.6}$$

where $\mathcal{L} \equiv \mathcal{L}(\overline{H})$ depends on the fixed point solution $\overline{H}$. To solve (1.6), we write P as a superposition of eigenfunctions P_j of the operator $\mathcal{L}$:

$$P(\xi) = \sum_{j=1}^{\infty} a_j(\tau) P_j(\xi), \tag{1.7}$$

where ν_j is the eigenvalue:

$$\mathcal{L}P_j = \nu_j P_j. \tag{1.8}$$

In the cases we know, the spectrum turns out to be discrete. For evolution PDEs involving second order elliptic differential operators, such as semilinear parabolic equations, mean curvature or Ricci flows, the discreteness of the spectrum of the linearization about the fixed point is a direct consequence of Sturm–Liouville theory [21, 22]. This theory establishes that, under quite general conditions on the coefficients of a second order linear differential operator and the boundary conditions, its spectrum is discrete and the corresponding eigenfunctions form a complete set in a suitably weighed L^2 space. Some explicit examples are presented in section 3.1.1. For general linear operators such a theory is not available, and one has to study the spectrum case by case.

Now the solution of (1.6) corresponding to P_j is

$$P = \mathrm{e}^{\nu_j \tau} P_j, \tag{1.9}$$

and all eigenvalues need to be negative for the similarity solution to be stable. In that case, convergence to the fixed point is exponential or *algebraic* in the original time variable t'. Soon the solution has effectively reached the fixed point, and there is very little change in the self-similar behaviour. If one or several of the eigenvalues around the fixed point vanish, the approach to the fixed point is slow, and the dynamics is effectively described by a dynamical system whose dimension corresponds to the number of vanishing eigenvalues. The same holds true if the attractor has few dimensions (such as a limit cycle or a low-dimensional chaotic attractor). Thus although singular behaviour is in principle a problem to be solved in infinite dimensions, in practice, it typically reduces to a dynamical problem of few dimensions. In this review we analyse singularities from the point of view of the *slow dynamics* contained in (1.4), to obtain an overview and tentative classification of possible scaling behaviour. We also emphasize the physical significance of these different types of behaviour.

The perspective described above suggests a close relationship to the description of scaling phenomena by means of the renormalization group, developed in the context of critical phenomena [23, 24]; we will continue to point out similarities, but we are not aware that a classification similar to ours has been achieved using the language of the renormalization group. For a computational perspective on analysing (1.4) in terms of its slow dynamics, see [25]. Finally, another approach sometimes associated with the classification of singularities is catastrophe theory [26]. However, as far as we are aware, catastrophe theory only yields useful results if the problem can be mapped onto a low-dimensional geometrical problem, which can in turn be rephrased in terms of normal forms of polynomials. This has been shown to be the case for wave problems such as shock formation and wave breaking [27], as well as singularities of the eikonal equation [28] and related problems [29].

In this paper we discuss the following cases:

(I) *Stable fixed points* (section 2)
In this case the fixed point is approached exponentially in the logarithmic variable τ, so the dynamics is described by the self-similar law (1.2). This pure power-law behaviour is also known as type-I self-similarity [30].

(II) *Centre manifold* (section 3)
Here one or more of the eigenvalues around the fixed point are zero. As a result, the approach to the fixed point is only algebraic, leading to logarithmic corrections to scaling. This is called type-II self-similarity [30]; it characterizes cases where the blow-up rate is different from what is expected on the basis of a solution of the type (1.2).

(III) *Travelling waves* (section 4)
Solutions of (1.1) converge to $h = t'^{\alpha}\phi(\xi + c\tau)$, which is a travelling wave solution of (1.4) with propagation velocity c.

(IV) *Limit cycles* (section 5)
Solutions have the form $h = t'^{\alpha}\psi[\xi, \tau]$ with ψ being a periodic function of period T in τ. This is known as 'discrete self-similarity' [15, 31], since at times $\tau_n = \tau_0 + nT$, n integer, the solution looks like a self-similar one.

(V) *Strange attractors* (section 6)
The dynamics on scale τ are described by a nonlinear (low-dimensional) dynamical system, such as the Lorenz equation.

(VI) *Multiple singularities* (section 7)
Blow-up may occur at several points (x_0, t_0) (or indeed in any set of positive measure), in which case the description (1.4) is not useful. We also describe cases where (1.2) still applies, and blow-up occurs at a single point, but the underlying dynamics is really one of two singularities which merge at the singular time.

Table 1. A summary of PDEs discussed in this paper. The first column gives the PDE in question, the second the type of dynamics near the fixed point according to the classification enumerated above. In the case of attracting fixed point dynamics, it is classed as 'stable', otherwise the equation governing the slow dynamics is given.

Equation	Type	Dynamics	Section
Free surface flow			
$h_t + \nabla\cdot(h^n\nabla\triangle h) \pm \nabla(h^p\nabla h) = 0$	I, II	Stable?	2.1.1
$(h^2)_t + (h^2u)_x = 0$	I		
$\rho(u_t + uu_x) = (h^2u_x)_x/h^2 - (h^{-1})_x$		Stable	2.1.1
$h_t = [h\kappa_x/(1+h_x^2)^{1/2}]_x,$	I		
$\kappa = 1/(h(1+h_x^2)^{1/2}) - h_{xx}/(1+h_x^2)^{3/2}$		Stable	2.1
$h_t + (hu)_x = 0,\ u_t + uu_x = h_{xxx}$	I	Stable	2.4.2
$\displaystyle\int \frac{\ddot a(\xi,t)\,\mathrm{d}\xi}{\sqrt{(x-\xi)^2+a(x,t)}} = \frac{\dot a^2}{2a}$	II	$v_\tau = -v^3$	3.2.1
$\displaystyle u(x) = \frac{1}{4}\int \frac{h_z(z)}{\sqrt{h^2(z)+(x-z)^2}}\,\mathrm{d}z$			
$(h^2)_t + (h^2u)_x = 0$	III	Stable	4
Geometric evolution equations			
$h_t = h_{zz}/(1+h_z^2) - 1/h$	II	$u_\tau = -u^2$	3.1.1
$\psi_t = \psi_{ss} - (n-1)(1-\psi_s^2)/\psi$	II	$u_\tau = -u^2$	3.1.1
Reaction–diffusion equations			
$u_t - \triangle u = f(u)$	II	$u_\tau = -u^2$	3.1.2
$u_t - \nabla\cdot(\lvert u\rvert^m\nabla u) = u^p$	II	Unknown	3.1.2
$\rho_t + \nabla\cdot(\rho\nabla S - \nabla\rho) = 0, \quad \rho = -\triangle S$	II	$u_\tau = -u^3$	3.2.2
Nonlinear dispersive equations			
$u_t + uu_x = 0$	I	Stable	2.4
$\mathrm{i}\psi_t + \triangle\psi + \lvert\psi\rvert^p\psi = 0$	I, II	$u_\tau = -u^2/v$	
		$v_\tau = -uv$	3.3
$u_t + u^pu_x + u_{xxx} = 0$	II	Unknown	3.3.1
$u_t - u_{xxt} + 3uu_x = 2u_xu_{xx} + uu_{xxx}$	I	Unknown	3.3.1
$u_t = 2fv,\ v_t = -2fu, f_t = f^2$	IV	Circle	5
Choptuik equations	I, IV	Limit cycle	5
$u_{tt} = u_{xx} + \lvert u\rvert^pu$	I, II	Unknown	7.2
Fluid equations			
$u_t + (u\cdot\nabla)u = -\nabla p + \triangle u,\ \nabla\cdot u = 0$	I, IV?	Unknown	2.2
$u_t + (u\cdot\nabla)u = -\nabla p,\ \nabla\cdot u = 0$	I, IV?	Unknown	2.2
$u_t + uu_x + vu_y = -p_x + u_{yy},\ u_x + v_y = 0$	I	Stable	2.2

This paper's aim is to assemble the body of knowledge on singularities of equations of the type (1.1) that is available in both the mathematical and the applied community, and to categorize it according to the types given above. In addition to rigorous results we pay particular attention to various phenomenological aspects of singularities which are often crucial for their appearance in an experiment or a numerical simulation. For example, what are the observable implications of the convergence onto the self-similar form (1.2) being slow? In most cases, we rely on known examples from the literature, but the problem is almost always reformulated to conform with the formulation advocated above. However, some examples are entirely new, which we will indicate as appropriate. For each of the above categories, we will present at least one example in greater detail, so the analysis can be followed explicitly. A concise overview of the equations presented in this review is given in table 1.

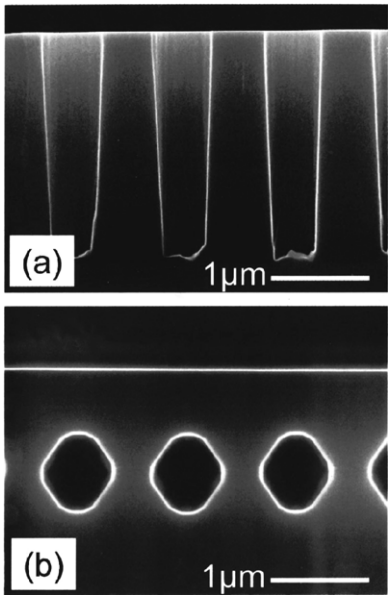

Figure 2. SEM images illustrating the pinch-off of a row of rectangular troughs in silicon (top) [36]. The bottom picture shows the same sample after 10 min of annealing at 1100 °C. The troughs have pinched off to form a row of almost spherical voids. The dynamics is driven by surface diffusion. Reprinted with permission from [36]. Copyright 2000, American Institute of Physics.

2. Stable fixed points

A sub-classification into self-similarity of the *first and second kinds* has been expounded in [32–35]. Self-similar solutions are of the first kind if (1.2) only solves (1.1) for one set of exponents α, β; their values are fixed by either dimensional analysis or symmetry and are thus rational. Solutions are of the second kind if solutions (1.2) exist *locally* for a continuous set of exponents α, β; however, in general these solutions are inconsistent with the boundary or initial conditions. Imposing these conditions leads to a nonlinear eigenvalue problem, whose solution yields irrational exponents in general.

2.1. Self-similarity of the first kind

Our example, exhibiting self-similarity of the first kind [35], is that of a solid surface evolving under the action of surface diffusion. Namely, atoms migrate along the surface driven by gradients of chemical potential, see figure 2. The resulting equations in the axisymmetric case, where the free surface is described by the local neck radius $h(x, t)$, are [37]

$$h_t = \frac{1}{h}\left[\frac{h}{(1+h_x^2)^{1/2}}\kappa_x\right]_x, \tag{2.1}$$

where

$$\kappa = \frac{1}{h(1+h_x^2)^{1/2}} - \frac{h_{xx}}{(1+h_x^2)^{3/2}} \tag{2.2}$$

is the mean curvature. In (2.1) and (2.2), all lengths have been made dimensionless using an outer length scale R (such as the initial neck radius), and the time scale R^4/D_4, where D_4 is a fourth-order diffusion constant.

Table 2. A series of similarity solutions of (2.4) as given in [43]. The higher-order solutions become successively thinner and flatter.

i	$H_i(0)$	c_i
0	0.701 595	1.037 14
1	0.636 461	0.298 66
2	0.456 842	0.183 84
3	0.404 477	0.134 89
4	0.355 884	0.107 30
5	0.326 889	0.089 42

Physically, it is important to point out that (2.1) describes the evolution of the free surface at elevated temperatures, above the so-called roughening transition. This implies that the solid surface is smooth and does not exhibit facets, coming from the underlying crystal structure. Above the roughening transition, a continuum description is still possible [38]. The study of these models has led to a number of interesting similarity solutions describing singular behaviour of the surface, such as grooves [39] or mounds [40, 41].

At a time $t' \ll 1$ away from breakup, dimensional analysis implies that $\ell = t'^{1/4}$ is a local length scale. This suggests the similarity form

$$h(x,t) = t'^{1/4} H(x'/t'^{1/4}), \tag{2.3}$$

and thus the exponents α, β of (1.2) are fixed by dimensional analysis, which is typical for self-similarity of the first kind. Of course, the result (2.3) also follows when directly searching for a solution of (2.1) in the form of (1.2). In other cases, a unique set of local scaling exponents is determined by symmetry [42]. The similarity form of the PDE becomes

$$-\frac{1}{4}(H - \xi H_\xi) = \frac{1}{H}\left[\frac{H}{(1+H_\xi^2)^{1/2}}\kappa_\xi\right]_\xi, \qquad \xi = \frac{x'}{t'^{1/4}} \tag{2.4}$$

where κ is the mean curvature of H.

Solutions of (2.4) have been studied extensively in [43]. To ensure matching to a time-independent outer solution, the leading order time dependence must drop out from (2.3), implying that

$$H(\xi) \sim c|\xi|, \qquad \xi \to \pm\infty; \tag{2.5}$$

the general form of this matching condition for self-similar solutions of the form (1.2) is

$$H(\xi) \sim c|\xi|^{\frac{\alpha}{\beta}}, \qquad \xi \to \pm\infty. \tag{2.6}$$

All solutions of the similarity equation (2.1) and which obey the growth condition (2.5) are symmetric, and form a discretely infinite set [43], similar to a number of other problems discussed below. The series of similarity solutions is conveniently ordered by descending values of the minimum, see table 2. Only the lowest order solution $H_0(\xi)$ is stable, and is shown in figure 3; we return to the issue of stability in section 2.5. The fact that permissible similarity solutions form a discrete set implies a great deal of 'universality' in the way pinching can occur. It means that the local solution is independent of the outer solution, and rather that the former imposes constraints on the latter; in particular, the prefactor c in (2.5) must be determined as part of the solution (see table 2).

2.1.1. Thin films and thin jets. A further class of solutions displaying self-similarity of the first kind is the generalized long-wave thin-film equation

$$h_t + \nabla \cdot (h^n \nabla \Delta h - B h^m \nabla h) = 0, \qquad n > 0. \tag{2.7}$$

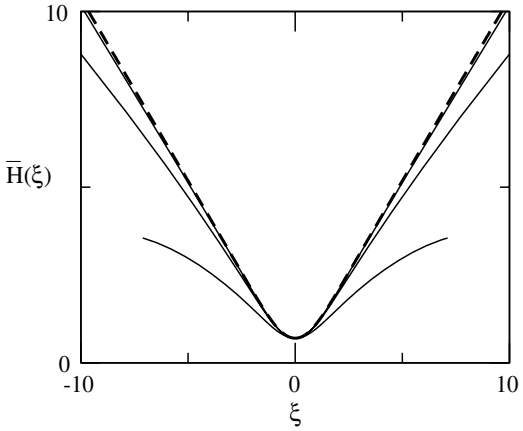

Figure 3. The approach to the self-similar profile for equation (2.1). The dashed line is the stable similarity solution $H(\xi)$ as found from (2.4). The full lines are rescaled profiles found from the original dynamics (2.1) at $h_m = 10^{-1}, 10^{-2}$ and $h_m = 10^{-3}$, respectively. As the singularity is approached, they converge rapidly onto the similarity solution (2.3).

The mass flux in this equation has two contributions: the first is due to surface tension and the second is due to an external potential. When $n = m = 3$, then $z = h(\boldsymbol{x}, t)$ represents the height of a film or a drop of viscous fluid over a flat surface, located at $z = 0$; the external potential is gravity. If B is negative, (2.7) describes a film that is hanging from a ceiling. Regardless of the sign of B, there is no singularity in this case [44]. The case $n = 1$ and $B = 0$ corresponds to flow between two solid plates, to which we return in section 7.1.

Solutions to (2.7) are said to develop point singularities if h goes to zero in finite time. This happens if one incorporates van der Waals forces, which at leading order implies $n = 3$ and $m = -1$ with $B < 0$. In [45, 46] (see also the review [47], where further full numerical simulations and mathematical theory are reported) the existence of radially symmetric self-similar touchdown solutions of the form

$$h(r, t) = t'^{\frac{1}{5}} H(\xi), \qquad \xi = r/t'^{\frac{2}{5}} \tag{2.8}$$

is shown numerically in this case. Self-similar solutions that touch down along a line exist as well, but they are unstable. A proof of formation of singularities in this context has been provided by Chou and Kwong [48].

A related set of equations is those for thin films and jets, but which are isolated instead of being in contact with a solid. Problems of this sort furnish many examples of type-I scaling, as reviewed from a physical perspective in [49]. If the motion is no longer dampened by the presence of a solid, inertia often has to be taken into account. This means that a separate equation for the velocity is needed, which is essentially the Navier–Stokes equation below, but often simplified by a reduction to a single dimension. Thus one has solutions of the form

$$h(x, t) = t'^{\alpha} H(\xi), \qquad u(x, t) = t'^{\beta-1} U(\xi), \tag{2.9}$$

where $\xi = x'/t'^{\beta}$. If $\alpha > \beta$ the profile is slender, and the dynamics is well described in a shallow-water theory. In this case the equations for an axisymmetric jet with surface tension become

$$\partial_t h^2 + \partial_x (u h^2) = 0 \tag{2.10}$$

and

$$\rho(\partial_t u + u \partial_x u) = -(\gamma/\rho)\partial_x (1/h) + 3\nu \frac{\partial_x (\partial_x u h^2)}{h^2}. \tag{2.11}$$

System (2.10) and (2.11) is interesting because it exhibits different scaling behaviour depending on the balance between the three different terms in (2.11) [42]. This is an illustration of the principle of *dominant balance*, which is of great practical importance in practice, where it is *a priori* not known which physical effect will be dominant. In the case of (2.11), these are the forces of inertia on the left, surface tension (first term on the right) and viscosity (second term on the right). Pinching is driven by surface tension, so it must always be part of the balance. Three different possible balances remain [42]:

(i) In the first case [50], all forces in (2.11) are balanced as the singularity is approached. The exponents $\alpha = 1, \beta = 1/2$ in (2.9) follow directly from this condition. As shown in [51], there is a discretely infinite sequence of self-similar profiles $H(\xi), U(\xi)$ corresponding to this balance. Numerical evidence strongly suggests that only the first profile, corresponding to the thickest thread, is stable [6]. All the other profiles are unstable, and thus cannot be observed. We will revisit this general scenario below, when we study the stability of fixed points more generally.
(ii) The second possibility corresponds to a balance between surface tension and viscous forces, thus putting $\rho = 0$ in (2.11). Physically, this occurs if the fluid is very viscous [52]. In section 2.4.1 we will describe the pinching solution corresponding to this case in more detail, as an example of self-similarity of the second kind. The exponent $\alpha = 1$ is fixed by the balance, but β is fixed only by an integrability condition. This once more results in an infinite sequence of solutions, ordered by the value of β. Again, only one profile, which has the largest value of $\beta = 0.174\,87$, is stable. This time, this corresponds to the smallest value of the minimum radius R_0, or the thinnest thread, as opposed to the thickest thread in the case of the inertial–surface tension–viscous balance.

If one inserts this viscous solution into the original equation (2.11), one finds that in the limit $t' \to 0$, the inertial term on the left grows faster than the two terms on the right. This means that regardless of how large the viscosity, eventually all three terms become of the same order, and one observes a crossover to the inertial–surface tension–viscous similarity solution described above, which is characterized by another set of scaling exponents and similarity profiles. In particular, the surface tension–viscous solution is symmetric about the pinch point, whereas the solution containing inertia is highly asymmetric [53]. We note that crossover between different similarity solutions may also occur by another mechanism, not directly related to the dominant balance between different terms in the equation (cf section 7.1).

Equations (2.10) and (2.11) correspond to a viscous liquid, surrounded by a gas, which is not dynamically active. The case of an external viscous fluid is considered in detail in section 4. The case of no internal fluid is special, in that the dynamics decouples completely into one for independent slices [54]. As a result, there is no universal profile associated with the breakup of a bubble in a viscous environment, but rather it is determined by the initial conditions.
(iii) At very low viscosity ($\nu \approx 0$ in (2.11)), the relevant balance is one where inertia is balanced by surface tension, so one might want to set $\nu = 0$ in (2.11), as done originally in [55]. However, the resulting equations do not lead to a selection of the values of the scaling exponents α, β; instead, there is a continuum of solutions [56], parametrized by the value of α, each with a continuum of possible similarity profiles. In fact, for vanishing viscosity (2.10) and (2.11) do not go towards a pinching solution, but the slope of the interface steepens, and one finds a shock solution [57], similar to the generic scenario described in section 2.4.

It was however shown numerically in [58, 59], and investigated in more detail in [60], that pinch-off of an inviscid fluid is well described by a solution of the full three-dimensional, axisymmetric potential flow equations. This is thus an example of a similarity solution of higher order in the independent variable, but both coordinate directions scale in the same way.

The scaling exponents in (2.9) are $\alpha = \beta = 2/3$ in this case, which violates the assumption $\alpha > \beta$ for the validity of the shallow-water equations (2.10) and (2.11). In addition, we note that the similarity profile can no longer even be written as a graph as assumed in (2.9), but *turn over*, as first observed experimentally in [61]. It is not known whether there also exists a *sequence* of similarity solutions, as in the case of the other balances. The case of no internal fluid is again very special, and leads to type-II scaling. It is considered in section 3.2.1.

Finally, variations of (2.10) and (2.11) have been investigated in [62]. Breakup was considered in arbitrary dimensions d (yet retaining axisymmetry) and with the pressure term $1/h$ replaced by an arbitrary power law $1/h^p$. After introducing a new variable $1/h^p$, there remains a single parameter $r = (d-1)/p$, which can formally be varied continuously. For all values of r, discrete sequences of type-I solutions are obtained. For $r > 1/2$, profiles are asymmetric, while below that value they are symmetric. At the critical value, both types of solutions coexist. Another interesting feature of the limit $r = 1/2$ is that the viscous term becomes subdominant at leading order. However, similar to the case $d = 3$, $p = 1$ mentioned above, no selection takes place in the absence of the viscous term. Nevertheless, the solutions selected by the presence of the viscous term are very close to an appropriately chosen member of the family of inviscid solutions.

2.2. Singularities in Euler and Navier–Stokes equations

One of the most important open problems, both in physics and mathematics, is the existence of singularities in the equations of fluid mechanics: Euler and Navier–Stokes equations in three space dimensions. The Navier–Stokes equations represent the evolution of a viscous incompressible fluid and are of the form

$$\boldsymbol{u}_t + \boldsymbol{u} \cdot \nabla \boldsymbol{u} = -\nabla p + Re^{-1} \Delta \boldsymbol{u}, \qquad \nabla \cdot \boldsymbol{u} = 0, \tag{2.12}$$

where $\boldsymbol{u}$ represents the velocity field, p the pressure in the fluid and Re is a dimensionless parameter called Reynolds number. Formally, by making $Re \to \infty$, the term involving $\Delta \boldsymbol{u}$ vanishes and we arrive at the Euler system, that models the evolution of the velocity and pressure fields of an inviscid incompressible fluid:

$$\boldsymbol{u}_t + \boldsymbol{u} \cdot \nabla \boldsymbol{u} = -\nabla p, \qquad \nabla \cdot \boldsymbol{u} = 0. \tag{2.13}$$

We exclude from our discussion certain 'exact' blow-up solutions of the Euler equations [63], which have the defect that the velocity goes to infinity *uniformly* in space; in other words, they lack the crucial mechanism of *focusing*. Formally, they are of course similarity solutions of (2.13), but with spatial exponent $\alpha = 0$.

As we mentioned above, the existence of singular solutions is unknown. Nevertheless, some scenarios have been excluded. For the Navier–Stokes equations, there exists no non-trivial self-similar solution of the first kind

$$\boldsymbol{u}(\boldsymbol{x}, t) = t'^{-1/2} \boldsymbol{U}(\boldsymbol{\xi}), \qquad \boldsymbol{\xi} = \boldsymbol{x}'/t'^{1/2} \tag{2.14}$$

in $L^2(\mathbb{R}^3)$. This was proved by Necas *et al* [64]. However, this does not exclude the formation of a singularity in a localized region: the matching condition (2.6) for this case implies $|\boldsymbol{U}| \propto |\xi|^{-1}$ as $|\xi| \to \infty$, which is *not* in L^2. Therefore, the theorem [64] does not apply.

A possible self-similar solution consisting of two skewed vortex pairs has been proposed by Moffatt in [7] in the spirit of the scenario suggested by the numerical simulations of Pelz [65], of the implosion of six vortex pairs in a configuration with cubic symmetry. A more recent numerical experiment by Hou and Li [66] seems to indicate that, although the velocity field may grow to very large values, singularities in the above-mentioned scenarios eventually saturate

and the solutions remain smooth. It has been argued in [67] that no self-similar solutions for Euler system should exist and that the 'limit-cycle' scenario described in section 5 could apply.

Under certain circumstances, such as special symmetry conditions or appropriate asymptotic limits, the Navier–Stokes and Euler systems may simplify and give rise to models for which the question of existence of singular solutions is somewhat simpler to analyse. This is the case for the Prandtl boundary-layer equations for the 2D evolution of the velocity field (u, v) in $y \geqslant 0$:

$$u_t + uu_x + vu_y = -p_x + u_{yy}, \qquad u_x + v_y = 0 \tag{2.15}$$

with boundary conditions $u = v = 0$; p is a given pressure field and the behaviour of the velocity field at infinity is prescribed. Equation (2.15) describes the asymptotic limit of the Navier–Stokes equation near a solid body in the limit of large Reynolds numbers Re. The variable x measures the arclength along the body, and $Re^{1/2}y$ is the distance from the body. Historically, a lot of attention was focused on the *stationary* version of (2.15), considering it as an evolution equation in x. At some position x_s along the body, the so-called Goldstein singularity $v \propto (x_s - x)^{-1/2}$ is encountered [68], which signals separation of the flow from the body. However, in reality the outer flow changes as a result of the appearance of a stagnation point, and one has to consider the *interaction* between the boundary layer and the outer flow [69].

It is thus conceptually simpler to consider the case of *unsteady* boundary-layer separation, which is described by the first singularity of (2.15) at time t_0. The formation of singularities of (2.15) in finite time was proved by E and Engquist [70]. It was first found numerically by van Dommelen and Shen [71], and its analytical structure was investigated in [72], using Lagrangian variables, which follow fluid particles as they separate from the surface (see also [73]). In the original Eulerian variables, the self-similar structure is [74, 75]

$$u = -u_0 + t'^{1/2}\phi_0^{1/2}U(\xi, \eta), \qquad \xi = \frac{x' - u_0 t'}{t'^{3/2}\phi_0^{1/2}}, \quad \eta = \frac{y\phi_0^{1/4}}{t'^{1/4}\Lambda}, \tag{2.16}$$

where u_0, ϕ_0 and Λ are constants which depend on the problem, while U is universal and can be given in terms of elliptic integrals. Note that the exponents for u and x are the generic exponents for a developing shock (see section 2.4), while the similarity exponent in the y-direction is different from the scaling for two-dimensional breaking waves [27]. We stress that the appearance of a singularity in (2.15) does not mean that the full 2D Navier–Stokes equation has developed a singularity. Instead, lower order terms in the asymptotic expansion that lead to (2.15) become important close to the singularity.

In relation to singularities in fluid mechanics, we can mention briefly a few important problems involving models or suitable approximations to the original Euler and Navier–Stokes systems. One concerns weak solutions to the Euler system for which the vorticity ($\omega = \nabla \times \boldsymbol{u}$) is concentrated in curves or surfaces. This is the case of the so-called vortex filaments and sheets in which the vorticity remains concentrated for all times, in the absence of viscosity. A useful way to represent the vortex sheet, when it evolves in 2D, is by assuming the location of its points $(x(\alpha, t), y(\alpha, t))$ as complex numbers $z(\alpha, t) = x(\alpha, t) + \mathrm{i}y(\alpha, t)$. Then, the evolution of $z(\alpha, t)$ is given by the so-called Birkhoff–Rott equation [76]:

$$z_t^*(\alpha, t) = \frac{1}{2\pi \mathrm{i}} PV \int_{-\infty}^{\infty} \frac{\gamma(z(\alpha', t), t)}{z(\alpha, t) - z(\alpha', t)} z_\alpha(\alpha', t)\, \mathrm{d}\alpha', \tag{2.17}$$

where z^* stands for the complex conjugate of z. The principal value is denoted by PV and γ is the vortex strength, which is such that $\mathrm{d}\Gamma = \gamma(z(\alpha, t), t)z_\alpha(\alpha, t)\, \mathrm{d}\alpha$ is constant along particle paths of the flow. The question then is whether or not these geometrical objects will

remain smooth at all times or develop singularities in finite time. In the case of vortex sheets, singularities are known to develop in the form of a divergence of the curvature at some point. These are called Moore's singularities after their observation and description by Moore [77]. A mathematical proof of existence of these singularities is provided by Caflisch and Orellana in [78]. These singularities exhibit self-similarity of the first kind as shown, for instance, in [79]: if one defines the inclination angle $\theta(s, t)$ in terms of the arclength parameter s as such that $z_s = \mathrm{e}^{\mathrm{i}\theta}$, then the curvature is given by $\kappa = \theta_s$ and may blow-up in the self-similar form (up to multiplicative constants):

$$\kappa(s, t') = \frac{1}{t'^{\delta}} g(\eta), \qquad \eta = s'/t', \quad 0 < \delta < 1, \tag{2.18}$$

where

$$g(\eta) = \frac{1}{(1+\eta^2)^{\frac{\delta}{2}}} \sin(\delta \arctan \eta) \, . \tag{2.19}$$

Interestingly, numerical simulations and Moore's original observations suggest that, although singular solutions with any δ are possible, the solution with $\delta = \frac{1}{2}$ is preferred. Thus the generically observed geometry near the singularity is of the form $y = |x|^{\frac{3}{2}}$, including the case of 3D simulations. This poses an interesting 'selection problem' for the $\frac{3}{2}$ power which has not received a definitive answer so far.

Another type of solution of (2.17) has the form of a double-branched spiral vortex sheet [80]. The explicit form is

$$z(\beta, t) = \begin{cases} t'^{q} \beta^{\nu} & \beta > 0, \\ t'^{q} |\beta|^{\nu} & \beta < 0, \end{cases} \tag{2.20}$$

where the two cases correspond to the two branches of the spiral. The parameter β is related to integration variable α of (2.17) by $\mathrm{d}\beta = z_\alpha \mathrm{d}\alpha$. The exponents are of the form $\nu = 1/2 + \mathrm{i}b$ and $q = 1/2 + \mathrm{i}\mu b$, corresponding to a vortex of radius $r = t'^{1/2}$ collapsing in finite time. However, in this case the vortex sheet strength is found to increase exponentially at infinity [80].

Vortex filaments result as the limit of a vortex tube when the thickness tends to zero. The fluid flow around a vortex filament is frequently approximated by a truncation of the Biot–Savart integral for the velocity in terms of the vorticity. This leads to a geometric evolution equation for the filament (see [81, chapter 7], and references therein) that can be transformed, via Hasimoto transformation, into the cubic nonlinear-Schrödinger in 1D. This fact allowed Gutierrez, Rivas and Vega to construct exact self-similar solutions for infinite vortex filaments [82]. One can also consider the vorticity concentrated in a region separating two fluids of different densities and in the presence of gravitational forces. This is the case of the surface water waves system for which the existence of singularities is open [83].

A different approach in the study of singularities for Euler and Navier–Stokes equations in three space dimensions relies on the development of models that share some of the essential mathematical difficulties of the original systems, but in a lower space dimension. This is the case of the surface quasi-geostrophic equation popularized by Constantin *et al* [84]:

$$\theta_t + \boldsymbol{v} \cdot \nabla\theta = 0, \tag{2.21a}$$

$$\boldsymbol{v} = \nabla^{\perp}\psi, \qquad \theta = -(-\triangle)^{1/2}\psi, \tag{2.21b}$$

to be solved in $d = 2$. This system of equations describes the convection of an active scalar θ, representing the temperature, with a velocity field which is an integral operator of the scalar itself. Nevertheless, the mere existence of singular solutions to this equation in the form of blow-up for the gradient of θ is still an open problem. One-dimensional analogues of this

problem, representing the convection of a scalar with a velocity field, which is the Hilbert transform of the scalar itself do have singularities in the form of cusps, as proved in [85, 86]. The structure of such singularities has been described in [87] and they are, in fact, of the type described in the next section, that is of the second kind.

2.3. Self-similarity of the second kind

In the example of the previous subsection, the exponents can be determined by dimensional analysis, or from considerations of symmetry, and therefore assume rational values. In many other problems, however, the scaling behaviour depends on external parameters, set for example by the initial conditions. In that case, the scaling exponent can assume any value. Often, this value is fixed by a compatability condition, resulting in an irrational answer. We will call this situation self-similarity of the second kind [32, 35]. Since it is relatively rare that results are tractable analytically, we mention two simple examples for which this is possible, although they do not come from time-dependent problems.

The first example is that of viscous flow near a solid corner of opening angle 2α [88]. For analogues of this problem in elasticity, see [89, 90] as well as the discussion in [35]. This flow is described by a Stokes' equation, whose solution near the corner is expected to be

$$\psi = r^{\lambda} f_{\lambda}(\theta). \tag{2.22}$$

If one of the boundaries is moving, scaling is of the first kind, and $\lambda = 2$ (the so-called Taylor scraper [91]). However, if the flow is driven by two-dimensional stirring at a distance from the corner, λ is determined by the transcendental equation

$$\sin 2(\lambda - 1)\alpha = -(\lambda - 1)\sin 2\alpha. \tag{2.23}$$

If $2\alpha < 146^{\circ}$, (2.23) admits complex solutions, which correspond to an infinite sequence of progressively smaller corner eddies. Since λ is complex, the strength of the eddies decreases as one comes closer to the corner.

The second example consists of calculating the electric field between two non-conducting spheres, where an external electric field is applied in the direction of the symmetry plane [92]. In this case the electric potential between the spheres is proportional to $(\rho/(Rh))^{\sqrt{2}-1}$, where ρ is the radial distance from the symmetry axis, R the sphere radius and h the distance between the spheres. Thus in accordance with the general ideas of self-similarity of the second kind, the singular behaviour is not controlled by the local quantity ρ/h, but the 'outer' parameter R comes into play as well. We now explain two analytically tractable *dynamical* examples of self-similarity of the second kind.

2.4. Breaking waves in conservation laws

We only consider the simplest model for the formation of a shock wave in gas dynamics, which is Burger's equation

$$u_t + uu_x = 0. \tag{2.24}$$

It is generally believed that any system of conservation laws that exhibits blow up will locally behave like (2.24) [94]. For example, figure 4 shows the steepening of a density wave in a gas, leading to a jump of the density in the picture on the right. In the words of [93]: 'We conclude that an infinite slope in the theoretical solution corresponds to a shock in real life'. As throughout this review, we only consider the dynamics up to the singularity. Which structure emerges after the singularity depends on the regularization used, as the continuation to times after the singularity is not unique [95, 96]. If the regularization is diffusive, a shock wave

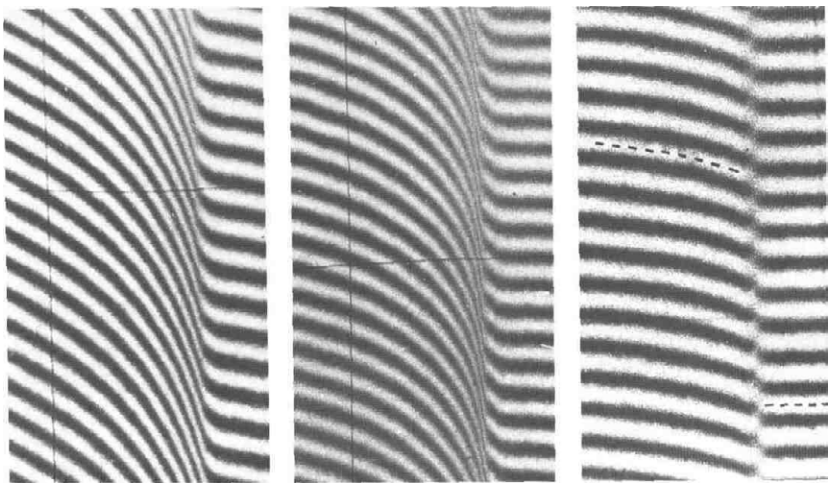

Figure 4. Fringe pattern showing the steepening of a wave in a gas, leading to the formation of a shock, which is travelling from left to right [93]. The vertical position of a given fringe is proportional to the density at that point. In the last picture a jump of seven fringes occurs. Reprinted with permission from [93]. Copyright 1954, American Association of Physics Teachers.

forms [97]; if it is a third derivative, one finds a KDV soliton. Finally, regularization by higher-order nonlinearities has been considered in [27] as a model of wave breaking.

It is well known [98] that (2.24) can be solved exactly using the method of characteristics. This method consists of noting that the velocity remains constant along the characteristic curve

$$z = u_0(x)t + x, \tag{2.25}$$

where $u_0(x) = u(x, 0)$ is the initial condition. Thus

$$u(z, t) = u_0(x) \tag{2.26}$$

is an exact solution to (2.24), given implicitly.

It is geometrically obvious that whenever $u_0(x)$ has a negative slope, characteristics will cross in finite time and produce a discontinuity of the solution. This happens when $\partial z/\partial x = 0$, which will occur for the first time at the singularity time

$$t_0 = \min\left\{-\frac{1}{\partial_x u_0(x)}\right\}, \tag{2.27}$$

at a spatial position $x = x_m$. This means a singularity will first form at

$$x_0 = x_m - \frac{u_0(x_m)}{\partial_x u_0(x_m)}. \tag{2.28}$$

Since (2.24) is invariant under any shift in velocity, we can assume without loss of generality that $u_0(x_m) = 0$, and thus that $x_0 = x_m$. This means the velocity is zero at the singularity. We now analyse the formation of the singularity using the local coordinates x', t'. In [27], this was done by expanding the initial condition u_0 in x', and using (2.26), using ideas from catastrophe theory [26]. Here instead we use the similarity ideas developed in this paper.

The local behaviour of (2.24) near t_0 can be obtained using the scaling

$$u(x, t) = t'^{\alpha} U\left(x'/t'^{\alpha+1}\right), \tag{2.29}$$

which solves (2.24). The similarity equation becomes

$$-\alpha U + (1+\alpha)\xi U_\xi + U U_\xi = 0, \tag{2.30}$$

with implicit solution

$$\xi = -U - CU^{1+1/\alpha}. \tag{2.31}$$

The special case $\alpha = 0$ has the solution $U = -\xi$, which is inconsistent with the matching condition (2.6), and thus has to be discarded.

We are thus left with a continuum of possible scaling exponents $\alpha > 0$, as is typical for self-similarity of the second kind. A discretely infinite sequence of exponents α_n is however selected by the requirement that (2.31) defines a smooth function for all ξ. Namely, one must have $1 + 1/\alpha$ odd, or

$$\alpha_i = \frac{1}{2i+2}, \qquad i = 0, 1, 2 \ldots, \tag{2.32}$$

and we denote the corresponding similarity profile by U_i. The constant C in (2.31) must be positive, but is otherwise arbitrary. It is set by the initial conditions, which is another hallmark of self-similarity of the second kind. However, C can be normalized to 1 by rescaling x and U. We will see in section 2.5 that the solution with α_0,

$$u(x,t) = t'^{1/2} U_0\left(x'/t'^{3/2}\right), \tag{2.33}$$

is the only stable one, all higher-order solutions are unstable.

It is interesting to look at some possible exceptions to the form of blow-up given above, suggested by [94]:

$$u_t + uu_x = u^\sigma. \tag{2.34}$$

This equation is also solved easily using characteristics. For $\sigma \leqslant 2$ the blow-up is always of the form (2.33), for $\sigma > 2$ two different types of behaviour are possible. For small initial data $u_0(x)$, a singularity still forms like (2.33), but in addition u may also go to infinity. However, there is a boundary between the two types of behaviour [94], where the slope blows up at the same time that u goes to infinity. For this case, one expects all terms in (2.34) to be of the same order, giving

$$u(x,t) = t'^{\frac{1}{1-\sigma}} U(\xi)), \qquad \xi = x'/t'^{\frac{\sigma-2}{\sigma-1}}, \tag{2.35}$$

with similarity equation

$$\frac{U}{1-\sigma} + \frac{\sigma-2}{\sigma-1}\xi U_\xi = U^\sigma - UU_\xi. \tag{2.36}$$

The solution to (2.36) that has the right decay at infinity is

$$\xi = -\frac{1}{(\sigma-2)U^{\sigma-2}} \pm C\frac{\left(1-(\sigma-1)U^{\sigma-1}\right)^{\frac{\sigma-2}{\sigma-1}}}{U^{\sigma-2}}, \tag{2.37}$$

where $C > 0$ is an arbitrary constant. The + and − signs describe the solution to the right and left of $\xi^* = -(\sigma-1)^{\frac{\sigma-2}{\sigma-1}}/(\sigma-2)$, respectively. The special case $\sigma = 4$ is shown in figure 5. The similarity solution (2.37) is not smooth at its maximum; rather, its first derivative behaves like $U_\xi \propto (\xi - \xi^*)^{1/(\sigma-2)}$. This can be understood from the exact solution; in order for blow-up to occur at the same time that a shock is formed, the initial profile must already have a maximum with the same regularity as (2.37). Thus, the situation leading to (2.35) is a very special one, requiring very peculiar initial conditions.

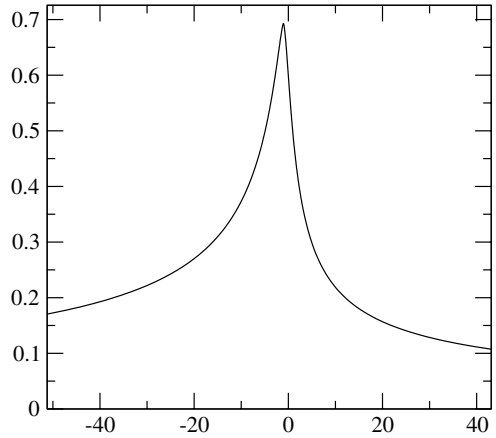

Figure 5. The similarity solution (2.37) for $\sigma = 4$.

2.4.1. Viscous pinch-off. As explained in section 2.1.1, the pinch-off of a very viscous fluid is described by (2.10) and (2.11), with $\rho = 0$, but only for finite range of scales. The equations can be simplified considerably by introducing *Lagrangian variables*, i.e. writing all profiles as a function of a particle label s. This means the particle is at position $z(s, t)$ at time t, and $z_t(s, t)$ is the velocity at time t. The jet profile can be obtained from $z_s = 1/h^2(s, t)$, and (2.11) becomes

$$h_t(s, t) = \frac{1}{6}\left(1 + \frac{C(t)}{h(s, t)}\right). \tag{2.38}$$

The typical velocity scale is γ/η, where γ is the surface tension and η is the viscosity; (2.38) has been made dimensionless accordingly. The time-dependent constant of integration $C(t)$ has to be determined self-consistently. Note that the self-similar form (1.2) is a solution of (2.38) for $\alpha = 1$, and *any* value of β; the exponent β will be determined by the consistency condition (2.45) below.

Since $\alpha = 1$, a scaling solution of (2.38) has the form

$$h^{-2}(s, t) = t'^{-2} f(\xi), \qquad \text{with} \quad \xi = s'/t'^{\gamma} \tag{2.39}$$

and

$$C(t) = -C_0 t'. \tag{2.40}$$

The relationship with the exponent β defined in (2.9) is simply $\beta = \gamma - 2$, as found from passing from Lagrangian to Eulerian variables. Inserting (2.39) and (2.40) into (2.38) we obtain

$$\frac{1}{\sqrt{f}} + 3\left(\frac{2}{f} + \frac{\gamma \xi f_\xi}{f^2}\right) = C_0, \tag{2.41}$$

where C_0 is a constant. Imposing symmetry and regularity of f, we expand $f(\xi)$ in the form

$$f_i(\xi) = R_0^{-2} + \xi^{2i+2} + O(\xi^{2i+4}), \qquad i = 0, 1, 2, \ldots \tag{2.42}$$

where we have normalized the coefficient of ξ^{2i+2} to one. This is consistent, since any solution of (2.38) is only determined up to a scale factor. Instead, the axial scale is fixed by the initial conditions. The parameter R_0 is the rescaled minimum of the profile: $h_m = R_0 t'$. Inserting (2.42) into (2.41), at order ξ^{2i+2} one obtains

$$R_0 = \frac{1}{12(\overline{\gamma} - 1)}, \qquad C_0 = \frac{1}{24}\frac{2\overline{\gamma} - 1}{(\overline{\gamma} - 1)^2}, \tag{2.43}$$

where we have put $\overline{\gamma} = (i + 1)\gamma$.

Each choice of i corresponds to one member in an infinite sequence of similarity solutions. Equation (2.41) can easily be integrated in terms of $\ln\xi$ and $y = \sqrt{f}$:

$$\int \frac{\mathrm{d}y}{\left((1+6R_0)\,y^3 - y^2 - 6R_0 y\right)} = \frac{1}{6R_0\gamma}\ln\xi + \widetilde{C} = \frac{1}{6R_0\overline{\gamma}}\ln\xi^{i+1} + \widetilde{C},$$

with $\widetilde{C}$ an arbitrary constant. Computing the integral above we obtain

$$y^{-\overline{\gamma}}\left((2\overline{\gamma}-1)\,y+1\right)^{\overline{\gamma}-\frac{1}{2}}(1-y)^{\frac{1}{2}} = \xi^{i+1}, \tag{2.44}$$

which is an implicit equation for the ith similarity profile $y \equiv y_i(\xi) = \sqrt{f_i(\xi)}$.

The value of the velocity U_∞ at infinity must be a constant to be consistent with boundary conditions. It can be found by integrating $z_{ts} = (h^{-2})_t = t'^{-3}(2f + \gamma\xi f_\xi)$ from zero to infinity:

$$U_\infty = \int_0^\infty z_{ts}\,\mathrm{d}s = \frac{t'^{\gamma-3}}{3}\int_0^\infty \left(\left(\frac{1}{24}\frac{2\overline{\gamma}-1}{(\overline{\gamma}-1)^2}\right)f^2 - f^{\frac{3}{2}}\right)\mathrm{d}\xi = 0, \tag{2.45}$$

where we have used (2.41). The above condition $U_\infty = 0$, which ensures that U_∞ does not diverge as $t' \to 0$, is the equation which determines the exponent γ. Taking the derivative of (2.44), we obtain

$$\begin{aligned}(i+1)\xi^i\frac{\mathrm{d}\xi}{\mathrm{d}y} &= \frac{\mathrm{d}}{\mathrm{d}y}\left(y^{-\overline{\gamma}}\left((2\overline{\gamma}-1)\,y+1\right)^{\overline{\gamma}-\frac{1}{2}}(1-y)^{\frac{1}{2}}\right)\\ &= -y^{-\overline{\gamma}-1}\left(2y\overline{\gamma}-y+1\right)^{\overline{\gamma}-\frac{3}{2}}\frac{\overline{\gamma}}{\sqrt{(1-y)}},\end{aligned}$$

which can be used to transform the integral in (2.45) to the variable y:

$$\begin{aligned}K_i(\gamma) \equiv \frac{3U_\infty}{(12(\overline{\gamma}-1))^3} = \frac{\overline{\gamma}}{i+1}\int_0^1 \left(\left(\frac{1}{2}\frac{2\overline{\gamma}-1}{\overline{\gamma}-1}\right)y^4 - y^3\right)\cdot\\ \left(y^{-\frac{i+1+\overline{\gamma}}{i+1}}\left((2\overline{\gamma}-1)\,y+1\right)^{-\frac{1}{2}\frac{2i-2\overline{\gamma}+3}{i+1}}(1-y)^{-\frac{1}{2}\frac{2i+1}{i+1}}\right)\mathrm{d}y = 0.\end{aligned} \tag{2.46}$$

The function $K_i(\gamma)$ may be written explicitly as

$$\begin{aligned}K_i(\gamma) = \gamma\frac{\Gamma(4-\gamma)\,\Gamma\left(\frac{1}{2i+2}\right)}{\Gamma\left(4-\gamma+\frac{1}{2i+2}\right)}\left(\frac{1}{2}\frac{(2i+2)\gamma-1}{(i+1)\gamma-1}\right)\cdot\\ F\left(\frac{2i+3}{2i+2}-\gamma, 4-\gamma; 4-\gamma+\frac{1}{2i+2}; 1-(2i+2)\gamma\right) - \gamma\frac{\Gamma(3-\gamma)\,\Gamma\left(\frac{1}{2i+2}\right)}{\Gamma\left(3-\gamma+\frac{1}{2i+2}\right)}\cdot\\ F\left(\frac{2i+3}{2i+2}-\gamma, 3-\gamma; 3-\gamma+\frac{1}{2i+2}; 1-(2i+2)\gamma\right),\end{aligned} \tag{2.47}$$

where $F(a, b; c, z)$ is the hypergeometric function [100]. Roots of γ_i are given in table 3.

To summarize, each exponent γ_i corresponds to a new member $f_i(\xi)$ of an infinite hierarchy of similarity profiles, to be found from (2.44). If one converts the Lagrangian variables back to the original spatial variables, one obtains

$$h(x,t) = t'\phi_{St}^{(n)}\left(x'/t'^{\gamma-2}\right). \tag{2.48}$$

Thus for $t' \to 0$ the typical radial scale t' of the generic $i = 0$ solution rapidly becomes smaller than the axial scale $t'^{0.175}$ (cf table 3). This explains the long necks seen in figure 6.

Table 3. A list of exponents, found from $K_i(\gamma) = 0$ using MAPLE, with K_i given by (2.47). The number $2i + 2$ gives the smallest non-vanishing power in a series expansion of the corresponding similarity solution around the origin. Only the solution with $i = 0$ is stable. The rescaled minimum radius is found from (2.43).

i	γ_i	R_0
0	2.1748	0.0709
1	2.0454	0.0797
2	2.0194	0.0817
3	2.0105	0.0825
4	2.0065	0.0828
5	2.0044	0.0832

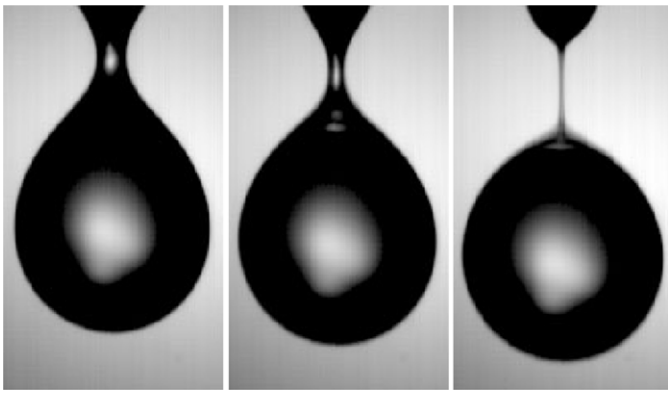

Figure 6. A drop of viscous fluid falling from a pipette 1 mm in diameter [99]. Note the long neck. Reproduced with permission from [99].

2.4.2. More examples. Other recent examples for scaling of the second kind have been observed for the breakup of a two-dimensional sheet with surface tension. In a shallow-water approximation, which is justified for a description of breakup, the equations read [101]

$$h_t + (hu)_x = 0, \qquad u_t + uu_x = h_{xxx} \tag{2.49}$$

after appropriate rescaling. Local similarity solutions can be found in the form

$$h(x,t) = t'^{4\beta-2}H(\eta), \qquad u(x,t) = t'^{\beta-1}U(\eta), \tag{2.50}$$

where $\eta = x'/t'^{\beta}$. The exponent β is not determined by dimensional analysis. Instead, it must be found from a solvability condition on the nonlinear system of equations for the similarity functions H, U.

The result of the numerical calculation is [101] $\beta = 0.6869 \pm 0.0003$, which is curiously close to $\beta = 2/3$, which is the value that had been conjectured earlier [102], but contains a small correction. The value $\beta = 2/3$ comes out if both length scales in the longitudinal and transversal directions are assumed to be the same, implying that $4\beta - 2 = \beta$. This is a natural expectation for problems governed by Laplace's equation, such as inviscid, irrotational flow [59], and indeed is observed for three-dimensional drop breakup [58, 59]. However, in the present case, even if the full two-dimensional irrotational flow equations are used, $\beta \neq 2/3$.

Other physical problems which frequently involve anomalous scaling exponents are strong explosions on the one hand, and collapse of particles or gases into a singular state on the other. These types of problems have been reviewed in great detail in a number of textbooks and papers

[32–35], but continue to attract a great deal of attention. As with many other singular problems, the type of scaling depends on the details of the underlying physics, and scaling of both the first and second kinds is observed. For example, the radius of a shock wave resulting from a strong explosion can be calculated from dimensional analysis to be $r_s \propto t^{2/5}$ [103]. However, in the seemingly analogous case of a strong *implosion*, an anomalous exponent is observed, which moreover depends on the parameters of the problem [98, 104]. Cases where collapse and shock formation coincide were given by [105] (similar to section 2.4). In a somewhat different context, anomalous scaling is observed in model calculations for the collapse of self-gravitating particles [106] and Bose–Einstein condensates [107]. It is important to remember that these examples come from *kinetic* equations describing the stochastic collision of waves or particles, and hence involving non-local collision operators. However, the kinetic equations appear to be closely related to certain PDE problems [108], which are analogous to other evolution equations studied in this paper.

2.5. *Stability of fixed points*

Self-similar solutions correspond to fixed points of the dynamical system (1.4), whose stability we now investigate by linearizing around the fixed point. We explain the situation for the example of section 2.1 in more detail, for which the transformation reads

$$h(x,t) = t'^{1/4} H(\xi,\tau), \tag{2.51}$$

where $\tau = -\ln(t')$. The similarity form of (2.1) becomes

$$H_\tau = \frac{1}{4}(H - \xi H_\xi) + \frac{1}{H}\left[\frac{H}{(1+H_\xi^2)^{1/2}}\kappa_\xi\right]_\xi, \tag{2.52}$$

which reduces to (2.4) if the left-hand side is set to zero. To assure matching of (2.52) to the outer solution, we have to require that (2.51) is to leading order time-independent as ξ is large, which leads to the boundary condition

$$H_\tau - (H - \xi H_\xi)/4 \to 0 \qquad \text{for} \quad |\xi| \to \infty. \tag{2.53}$$

This is the natural extension of (2.5) to the time-dependent case.

Next we linearize around any one of the similarity solutions $\overline{H}(\xi) = H_i(\xi)$ listed in table 2, as described in the introduction. The stability is controlled by eigenvalues of the eigenvalue equation (1.8). Inserting the eigensolution (1.9) into (2.53) one finds that P_j must grow at infinity like

$$P_j(\xi) \propto \xi^{1-4\nu_j}. \tag{2.54}$$

Similarly, the growth condition for the general case of a similarity solution of the form (1.2) is

$$P_j(\xi) \propto \xi^{\frac{\alpha-\nu_j}{\beta}}. \tag{2.55}$$

If the similarity solution $\overline{H}(\xi)$ is to be stable, the real part of the eigenvalues of $\mathcal{L}$ must be negative. However, there are always two positive eigenvalues, which are related to the invariance of the equation of motion (2.1) under translations in space and time, as noted by [109, 110]. Namely, for any ϵ, the translated similarity solution

$$h^{(\epsilon)}(x,t) = t'^{1/4}\overline{H}\left(\frac{x'+\epsilon}{t'^{1/4}}\right) \tag{2.56}$$

is an equally good self-similar solution of (2.1), and thus of (2.52). In particular, we can expand (2.56) to lowest order in ϵ, and find that

$$H^{(\epsilon)}(\xi,\tau) = \overline{H}(\xi) + \epsilon e^{\beta\tau}\overline{H}_\xi(\xi) + O(\epsilon^2), \tag{2.57}$$

where the linear term is a solution of (1.6).

Thus

$$\left(\mathrm{e}^{\beta\tau}\overline{H}_\xi\right)_\tau = \mathrm{e}^{\beta\tau}\beta\overline{H}_\xi = \mathrm{e}^{\beta\tau}\mathcal{L}\overline{H}_\xi. \tag{2.58}$$

But this means that $\nu_x = \beta \equiv 1/4$ is an eigenvalue of $\mathcal{L}$ with eigenfunction $\overline{H}_\xi(\xi)$. Similarly, considering the transformation $t \to t + \epsilon$, one finds a second positive eigenvalue $\nu_t = 1$, with eigenfunction $\xi\overline{H}_\xi$. However, these two positive eigenvalues *do not* correspond to instability. Instead, the meaning of these eigenvalues is that upon perturbing the similarity solution, the singularity time as well as the position of the singularity will change. Thus if the coordinate system is not adjusted accordingly, it looks as if the solution would flow away from the fixed point. If, on the other hand, the solution is represented relative to the perturbed values of x_0 and t_0, the eigenvalues ν_x and ν_t will not appear.

The eigenvalue problem (1.8) was studied numerically in [43]. It was found that each similarity solution $\overline{H}_i$ has exactly $2i$ positive real eigenvalues, *disregarding* ν_x, ν_t. The result is that the linearization around the 'ground state' solution $\overline{H}_0$ only has negative eigenvalues while *all* the other solutions have at least one other positive eigenvalue. This means that $\overline{H}_0$ is the only similarity solution that can be observed, all other solutions are unstable. Close to the fixed point, the approach to $\overline{H}_0$ will be dominated by the largest negative eigenvalue ν_1:

$$h(x,t) = t'^{1/4}\left[\overline{H}(\xi) + \epsilon t'^{-\nu_1}P_1(\xi)\right]. \tag{2.59}$$

For large arguments, the point ξ_{cr} where the correction becomes comparable to the similarity solution is $\xi \sim \epsilon t'^{-\nu_1}\xi^{1-4\nu_1}$, and thus $\xi_{cr} \sim t'^{-1/4}$. This means that the region of validity of $\overline{H}(\xi)$ *expands* in similarity variables, and is constant in real space. This rapid convergence is reflected by the numerical results reported in figure 3. More formally, one can say that for any ϵ there is a δ such that

$$\left|h(x,t) - t'^{1/4}\overline{H}(\xi)\right| \leqslant \epsilon \tag{2.60}$$

if $|x'| \leqslant \delta$ *uniformly* as $t' \to 0$.

We suspect that the situation described above is more general: the ground state is stable, while each following profile has a number of additional eigenvalues. In the case of the sequence of profiles $\overline{H}_i$ of (2.4), two new positive eigenvalues appear for each new profile, corresponding to a symmetric and an antisymmetric eigenfunction. Below we give two more examples of the same scenario, for which we are able to give a simple geometrical interpretation for the appearance of two additional positive eigenvalues at each stage of the hierarchy of similarity solutions. The simplest case is that of shock wave formation (cf section 2.4), for which everything can be worked out analytically.

The dynamical system corresponding to the self-similar solution (2.29) is

$$U_\tau - \alpha U + (1+\alpha)\,\xi U_\xi + UU_\xi = 0, \tag{2.61}$$

and so the eigenvalue equation for perturbations P around the base profile $\overline{U}_i$ becomes

$$(\alpha_i - \nu)P - (1+\alpha_i)\xi P_\xi - P(\overline{U}_i)_\xi - P_\xi\overline{U}_i = 0, \qquad i = 0, 1, \ldots \tag{2.62}$$

Here $\overline{U}_i$ is the ith similarity function defined by (2.31) for the exponents α_i as given by (2.32).

The eigenvalue equation (2.62) is easily solved by transforming from the variable ξ to the variable $\overline{U}$, using (2.31):

$$P\left[(\alpha_i - \nu)(1 + (2i+3)\overline{U}_i^{2i+2}) + 1\right] = \frac{\partial P}{\partial \overline{U}}\left[\alpha_i\overline{U}_i + (1+\alpha_i)\overline{U}_i^{2i+3}\right], \tag{2.63}$$

with solution

$$P = \frac{\overline{U}_i^{3+2i-2\nu(i+1)}}{1 + (2i+3)\overline{U}_i^{2i+2}}. \tag{2.64}$$

The exponent $3+2i-2\nu(i+1)$ must be an integer for (2.64) to be regular at the origin, so the eigenvalues are

$$\nu_j = \frac{2i+4-j}{2i+2}, \qquad j = 1, 2, \ldots \tag{2.65}$$

As usual, the eigensolutions are alternating between even and odd. However, we are interested in the *first* instance, given by (2.27), at which a shock forms. This implies that the second derivative of the profile must vanish at the location of the shock, and the amplitude of the $j = 3$ perturbation must be exactly zero.

Thus for $i = 0$ the remaining eigenvalues are $\nu = 3/2, 1, 0, -1/2, \ldots$; the first two are the eigenvalues $\nu_x = \beta = 1+\alpha$ and $\nu_t = 1$ found above. The vanishing eigenvalue occurs because there is a family of solutions parameterized by the coefficient C in (2.31). All the other eigenvalues are negative, which shows that the similarity solution (2.33) is stable. In the same vein, for $\alpha_1 = 1/4$ there are two more positive exponents: $\nu = 5/4, 1, 1/2, 1/4$, so the solution must be unstable. The same is of course true for all higher order solutions. Thus in conclusion the ground state solution $\overline{U}_0$ given by (2.33) is the only observable form of shock formation. The same conclusion was reached in [27] by a stability analysis based on catastrophe theory.

The sequence of profiles for viscous pinch-off, found in section 2.3, suggests a simple mechanism for the fact that two new unstable directions appear with each new similarity profile of higher order. In fact, the argument is strikingly similar to that given for shock formation. Differentiating (2.38) with respect to s one finds that a local minimum point $s_{\min}$ remains a minimum. Thus the local time evolution of the profile can be written as

$$h(s,t) = h_m + \sum_{j=2}^{\infty} B_j(t) s'^j. \tag{2.66}$$

For generic initial data $B_2(0) \neq 0$, so there is no reason why B_2 should vanish at the singular time, which means that the self-similar solution f_0 will develop, which has a quadratic minimum. This situation is structurally stable, so one expects the eigenvalues of the linearization to be negative. If however the coefficients $B_j(0)$ are zero for $j = 2, \ldots 2n-1$, they will remain zero for all times. Namely, if the first k s-derivatives of h vanish, one has

$$\partial_s^j h_t = -\frac{C\partial_s^j h}{h^2}, \qquad j = 1, \ldots, k, \tag{2.67}$$

so the first k derivatives will remain zero. Thus to find the similarity profile with $i = 1$, one needs $B_2(0) = B_3(0) = 0$ as an initial condition. This is a non-generic situation, and a slight perturbation will make B_2 and B_3 non-zero. In other words, there are two unstable directions, which take the solution away from $f_1(\xi)$, as defined by (2.42). In the general case, the linearization around $f_i(\xi)$ will have $2i$ positive eigenvalues (apart from the trivial ones). Extensive numerical simulations of drop pinch-off in the inertial–surface tension–viscous regime (cf section 2.1.1) suggests that the hierarchy of similarity solutions again has similar properties in this case as well, although stability has not been studied theoretically. The ground state profile is stable, while all the others are unstable [42]. Even when using a higher-order similarity solution as an initial condition, it is immediately destabilized, and converges onto the ground state solution [51].

3. Centre manifold

In section 2 we described the generic situation that the behaviour of a similarity solution is determined by the linearization around it. In the case of a stable fixed point, convergence is

exponentially fast, and the observed behaviour is essentially that of the fixed point. In this section, we describe a variety of cases where the dynamics is slow. In all cases we are able to associate this slow dynamics with a fixed point in the appropriate variable(s), around which the eigenvalues vanish. Instead, higher-order nonlinear terms have to be taken into account, and the slow approach to the fixed point is determined by a low-dimensional dynamical system.

We consider essentially two different cases:

(a) The dynamical system (1.4) possesses a fixed point $H_0(\xi)$, which has a *vanishing* eigenvalue, with corresponding eigenfunction $\psi(\xi)$. The dynamics in the slow direction ψ is described by a nonlinear equation for the amplitude $a(\tau)$, which varies on a logarithmic time scale:

$$h = t'^{\alpha}\left[H_0(\xi) + a(\tau)\psi(\xi)\right], \qquad \xi = x'/t'^{\beta}. \tag{3.1}$$

(b) The dynamical system does not possess a fixed point, but has a solution of a slightly more general form

$$h = h_0(\tau)H(\xi), \qquad \xi = x'/W(\tau), \tag{3.2}$$

where h_0 and W are not necessarily power laws. To expand about a fixed point, we define the generalized exponents

$$\alpha = -\partial_\tau h_0/h_0, \qquad \beta = -\partial_\tau W/W, \tag{3.3}$$

which now depend on time. In the case of a type-I similarity solution, this reduces to the usual definition of the exponent. In the cases considered below, one derives a finite dimensional dynamical system for the exponents α, β (potentially including other, similarly defined scale factors). Once more, the exponents vary on a logarithmic time scale, which can be understood from the fact that the dynamical system possesses a fixed point with vanishing eigenvalues.

Zero eigenvalues can also be associated with symmetries of the singularity, like rotational or translational symmetries, which lead to the existence of a continuum of similarity solutions. Another example, which concerns the dynamics inside the singular object itself, is wave steepening as described by (2.31). As seen from (2.65), there indeed is a vanishing eigenvalue associated with this continuum of solutions. Below we will not be concerned with this case, but only consider approach to the singularity starting from non-singular solutions.

3.1. Quadratic nonlinearity: geometric evolution and reaction–diffusion equations

The appearance of this type of nonlinearity is characteristic for various nonlinear parabolic equations and systems. The blow-up behaviour is characterized by the presence of logarithmic corrections in the similarity profiles.

3.1.1. Geometric evolution equations: mean curvature and Ricci flows. Axisymmetric motion by mean curvature in three spatial dimensions is described by the equation

$$h_t = \left(\frac{h_{xx}}{1+h_x^2} - \frac{1}{h}\right), \tag{3.4}$$

where $h(x,t)$ is the radius of the moving free surface. A very good physical realization of (3.4) is the melting and freezing of a ^{3}He crystal, driven by surface tension [111], see figure 7. As before, the time scale t has been chosen such that the diffusion constant, which sets the rate of motion, is normalized to one. A possible boundary condition for the problem is that $h(0,t) = h(L,t) = R$, where R is some prescribed radius. For certain initial conditions

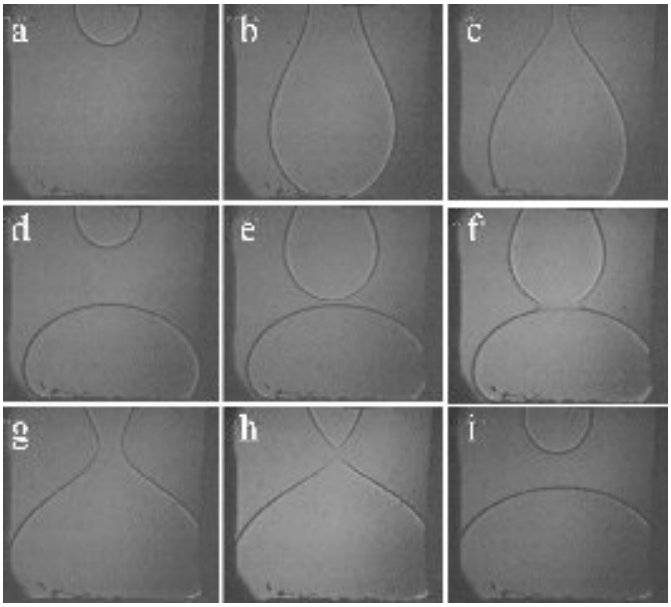

Figure 7. Nine images (of width 3.5 mm) showing how a ^{3}He crystal 'flows' down from the upper part of a cryogenic cell into its lower part [112]. The recording takes a few minutes, the temperature is just above the temperature $T_{\min} = 0.32$ K, where the latent heat vanishes. The crystal first 'drips' down, so that a crystalline 'drop' forms at the bottom ((*a*)–(*c*)); then a second drop appears (*d*) and comes into contact with the first one (*e*); coalescence is observed (*f*) and subsequently breakup occurs (*h*). Reprinted with permission from [112]. Copyright 1999, American Institute of Physics.

$h(x, 0) \equiv h_0(x)$ the interface will become singular at some time t_0, at which $h(x_0, t_0) = 0$ and the curvature blows up. The moment of blow-up is shown in panel (*h*) of figure 7, for example.

Inserting the self-similar solution (1.2) into (3.4), one finds a balance for $\alpha = \beta = 1/2$. The corresponding similarity equation is

$$-\frac{\phi}{2} + \xi\frac{\phi_\xi}{2} = \left(\frac{\phi_{\xi\xi}}{1+\phi_\xi^2} - \frac{1}{\phi}\right), \qquad \xi = \frac{x'}{t'^{1/2}}. \tag{3.5}$$

One solution of (3.5) is the constant solution $\phi(\xi) = \sqrt{2}$. Another potential solution is one that grows linearly at infinity, to ensure matching onto a time-independent outer solution. However, it can be shown that no solution to (3.5), which also grows linearly at infinity, exists [113, 114]. Our analysis below follows the rigorous work in [30], demonstrating type-II self-similarity. In addition, we now show how the description of the dynamical system can be carried out to arbitrary order.

The relevant solution is thus the constant solution, but which of course does not match onto a time-independent outer solution. We thus write the solution as

$$h(x, t) = t'^{1/2}\left[\sqrt{2} + g(\xi, \tau)\right], \tag{3.6}$$

with $\tau = -\ln(t')$ as usual. The equation for g is then

$$g_\tau = g - \frac{\xi g_\xi}{2} + \frac{g_{\xi\xi}}{1+g_\xi^2} - \frac{g^2}{2^{3/2}+2g}, \tag{3.7}$$

which we solve by expanding into eigenfunctions of the linear part of the operator

$$\mathcal{L}g = g - \xi g_\xi/2 + g_{\xi\xi}. \tag{3.8}$$

It is easily confirmed that

$$\mathcal{L}H_{2i}(\xi/2) = \nu_i H_{2i}(\xi/2), \qquad i = 0, 1, \ldots, \tag{3.9}$$

where H_n is the nth Hermite polynomial [100]:

$$H_n(y) = (-1)^n \mathrm{e}^{y^2} \frac{\mathrm{d}^n}{\mathrm{d}y^n} \mathrm{e}^{-y^2}, \tag{3.10}$$

and $\nu_i = 1 - i$. Thus the first eigenvalue is $\nu_0 = 1$, which corresponds to the positive eigenvalue ν_t coming from the arbitrary choice of t_0. The other positive eigenvalue ν_x does not appear, since we have chosen to look at symmetric solutions, breaking translational invariance. However, the largest non-trivial eigenvalue ν_1 is zero, and the linear part of (3.7) becomes

$$\frac{\partial a_i}{\partial \tau} = (1 - i)a_i, \qquad i = 0, 1, \ldots. \tag{3.11}$$

Thus all perturbations with $i > 1$ decay, but to investigate the approach of the cylindrical solution, one must include nonlinear terms in the equation for a_1.

If we write

$$g(\xi, \tau) = \sum_{i=1}^{\infty} a_i(\tau) H_{2i}(\xi/2), \tag{3.12}$$

the equation for a_1 becomes

$$\frac{\mathrm{d}a_1}{\mathrm{d}\tau} = -2^{3/2} a_1^2 + O(a_1 a_j), \tag{3.13}$$

whose solution is

$$a_1 = 1/(2^{3/2}\tau). \tag{3.14}$$

Thus instead of the expected exponential convergence onto the fixed point, the approach is only algebraic. Since all other eigenvalues are negative, the τ-dependence of the a_i is slaved by the dynamics of a_1. Namely, as we will see below, $a_j = O(\tau^{-j})$, so corrections to (3.13) are of higher order. To summarize, the leading order behaviour of (3.4) is given by

$$h(x, t) = t'^{1/2} \left[\sqrt{2} + a_1(\tau) H_2(\xi) \right], \tag{3.15}$$

as was proven by [30].

Now we compute the specific form of the higher-order corrections to (3.15), which have not been worked out explicitly before. If one linearizes around (3.14), putting $a_1 = a_1^{(0)} + \epsilon_1$, one finds

$$\frac{\mathrm{d}\epsilon_1}{\mathrm{d}\tau} = -\frac{2}{\tau}\epsilon_1 + \text{other terms}. \tag{3.16}$$

This means that the coefficient A of $\epsilon_1 = A/\tau^2$ remains undetermined, and a simple expansion of a_i in powers of τ^{-1} yields an indeterminate system. Instead, at quadratic order, a term of the form $\epsilon_1 = A \ln \tau/\tau^2$ is needed. Fortunately, this is the only place in the system of nonlinear equations for a_i where such an indeterminacy occurs. Thus all logarithmic dependences can be traced, leading to the general ansatz

$$a_i^{(n)} = \frac{\delta_i}{\tau^i} + \sum_{k=i+1}^{n} \sum_{l=0}^{k-i} \frac{(\ln \tau)^l}{\tau^k} \delta_{lki}, \tag{3.17}$$

where δ_i and δ_{lki} are coefficients to be determined. The index n is the order of the truncation.

The coefficients can now be found recursively by considering terms of successively higher order in τ^{-1} in the first equation:

$$\frac{da_1}{d\tau} = -2^{3/2}a_1^2 - 24\sqrt{2}a_1a_2 + 22a_1^3 - 272\sqrt{2}a_1^4 - 191\sqrt{2}a_2^2 + 192a_1^2a_2 \tag{3.18a}$$

$$\frac{da_2}{d\tau} = -a_2 - \sqrt{2}/4a_1^2 + 6a_1^3 - 8\sqrt{2}a_1a_2. \tag{3.18b}$$

The next two orders will involve the next coefficient a_3. From (3.18*a*) and (3.18*b*), one first finds δ_{121} and δ_2, by considering $O(\tau^{-3})$ and $O(\tau^{-2})$, respectively. Then, at order $O(\tau^{-(n+1)})$ in the first equation, where $n = 3$, one finds all remaining coefficients δ_{lki} in the expansion (3.17) up to $k = n$. At each order in τ^{-1}, there is of course a series expansion in $\ln\tau$ which determines all the coefficients.

We constructed a MAPLE program to compute all the coefficients up to arbitrarily high order (10th, say). Up to third order in τ^{-1} the result is

$$a_1 = 1/4\,\frac{\sqrt{2}}{\tau} + \frac{17}{16}\,\frac{\ln(\tau)\sqrt{2}}{\tau^2} - \frac{73}{16}\,\frac{\sqrt{2}}{\tau^3} + \frac{867}{128}\,\frac{\ln(\tau)\sqrt{2}}{\tau^3} - \frac{289}{128}\,\frac{(\ln(\tau))^2\sqrt{2}}{\tau^3} \tag{3.19a}$$

$$a_2 = -1/32\,\frac{\sqrt{2}}{\tau^2} + \frac{5}{16}\,\frac{\sqrt{2}}{\tau^3} - \frac{17}{64}\,\frac{\ln(\tau)\sqrt{2}}{\tau^3}, \tag{3.19b}$$

and thus $h(x,t)$ becomes

$$h(x,t) = t'^{1/2}\left[\sqrt{2} + a_1(\tau)\left(-2+\xi^2\right) + a_2(\tau)\left(12 - 12\xi^2 + \xi^4\right)\right], \tag{3.20}$$

from which one of course immediately finds the minimum. To second order, the result is

$$h_m = (2t')^{1/2}\left[1 - \frac{1}{2\tau} - \frac{3 + 17\ln\tau}{8\tau^2}\right]. \tag{3.21}$$

First, the presence of logarithms implies that there is some dependence on initial conditions built into the description. The reason is that the argument inside the logarithm needs to be non-dimensionalized using some 'external' time scale. More formally, any change in time scale $\tilde{t} = t/t_0$ leads to an identical equation if also lengths are rescaled according to $\tilde{h} = h/\sqrt{t_0}$. This leaves the prefactor in (3.21) invariant, but adds an arbitrary constant τ_0 to τ. This is illustrated by comparing with a numerical simulation of the mean curvature equation (3.4) close to the point of breakup, see figure 8. Namely, we subtract the analytical result (3.21) from the numerical solution $h_m/(2\sqrt{t'})$ and multiply by τ^2. As seen in figure 8, the remainder is varying slowly over 12 decades in t'. If the constant τ_0 is adjusted, this small variation is seen to be consistent with the logarithmic dependence predicted by (3.21).

The second important point is that convergence in space is no longer uniform as implied by (2.60) for the case of type-I self-similarity. Namely, to leading order the pinching solution is a cylinder. For this to be a good approximation, one has to require that the correction is small: $\xi^2/\tau \ll 1$. Thus corrections become important beyond $\xi_{cr} \sim \tau$, which, in view of the logarithmic growth of τ, implies convergence in a constant region *in similarity variables only*. As shown in [111], the slow convergence towards the self-similar behaviour has important consequences for a comparison with experimental data.

Mean curvature flow is also an example of a broader class of problems called generically 'geometric evolution equations'. These are evolution equations intended to gain topological insight by flowing geometrical objects (such as metric or curvature) towards easily recognizable objects such as constant or positive curvature manifolds. The most remarkable example is the so-called Ricci flow, introduced in [115], which is the essential tool in the recent proof of

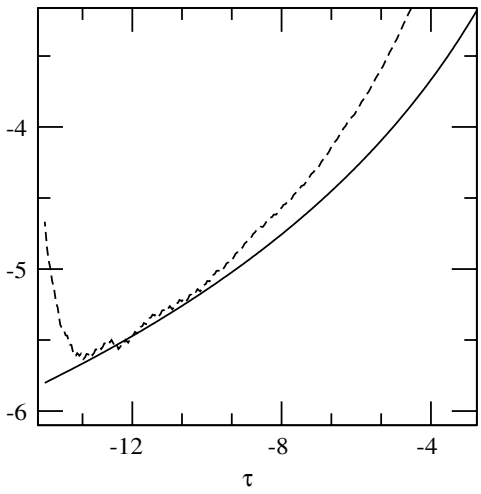

Figure 8. A plot of $[h_m/\sqrt{2t'} - 1 + 1/(2\tau)]\tau^2$ (dashed line) and $\tau_0/2 - (3 + 17\ln(\tau + \tau_0)/8)$ (full line) with $\tau_0 = 4.56$.

the geometrization conjecture (including Poincaré's conjecture as a consequence) by Grigori Perelman.

Namely, Poincaré's conjecture states that every simply connected closed 3-manifold is homeomorphic to the 3-sphere. Being homeomorphic means that both are topologically equivalent and can be transformed one into the other through continuous mappings. Such mappings can be obtained from the flow associated with an evolutionary PDE involving fundamental geometrical properties of the manifold. Thurston's geometrization conjecture is a generalization of Poincaré's conjecture to general 3-manifolds and states that compact 3-manifolds can be decomposed into submanifolds that have basic geometric structures.

Perelman sketched a proof of the full geometrization conjecture in 2003 using Ricci flow with surgery [116]. Starting with an initial 3-manifold, one deforms it in time according to the solutions of the Ricci flow PDE (3.22) we consider below. Since the flow is continuous, the different manifolds obtained during the evolution will be homeomorphic to the initial one. The problem is in the fact that Ricci flow develops singularities in finite time, one of which we describe below. One would like to get over this difficulty by devising a mechanism of continuation of solutions beyond the singularity, making sure that such a mechanism controls the topological changes leading to a decomposition into submanifolds, whose structure is given by Thurston's geometrization conjecture. Perelman obtained essential information on how singularities are like, essentially three dimensional cylinders made out of spheres stretched out along a line, so that he could develop the correct continuation (also called 'surgery') procedure and continue the flow up to a final stage consisting of the elementary geometrical objects in Thurston's conjecture.

Ricci flow is defined by the equation

$$\frac{\partial g_{ij}}{\partial t} = -2R_{ij} \tag{3.22}$$

for a Riemannian metric g_{ij}, where R_{ij} is the Ricci curvature tensor. The Ricci tensor involves second derivatives of the curvature and terms that are quadratic in the curvature. Hence, there is the potential for singularity formation and singularities are, in fact, formed. As Perelman poses it, the most natural way to form a singularity in finite time is by pinching an almost

round cylindrical neck. The structure of this kind of singularity has been studied in [117]. By writing the metric of a $(n+1)$-dimensional cylinder as

$$g = \mathrm{d}s^2 + \psi^2 g_{\mathrm{can}}, \tag{3.23}$$

where g_{can} is the canonical metric of radius one in the n-sphere S^n, $\psi(s,t)$ is the radius of the hypersurface $\{s\} \times S^n$ at time t and s is the arclength parameter of the generatrix of the cylinder.

The equation for ψ then becomes

$$\psi_t = \psi_{ss} - \frac{(n-1)(1-\psi_s^2)}{\psi}. \tag{3.24}$$

In [117] it is shown that for $n > 1$ the solution close to the singularity admits a representation that resembles the one obtained for mean curvature flow:

$$\psi(s,t) = \frac{1}{2^{\frac{1}{2}}(n-1)^{\frac{1}{2}} t'^{1/2}} u(\xi,\tau), \qquad \xi = s/t'^{1/2}. \tag{3.25}$$

Namely, (3.24) admits a constant solution $u(\xi,\tau) = 1$, and the linearization around it gives the same linear operator (3.8) as for mean curvature flow. Thus a pinching solution behaves as

$$u(\xi,\tau) = 1 + a(\tau) H_2(\xi/2) + o(\tau^{-1}), \tag{3.26}$$

where the equation for a is $a_\tau = -8a^2$, with solution $a = 1/(8\tau)$.

3.1.2. Reaction–diffusion equations. The semilinear parabolic equation

$$u_t - \Delta u - |u|^{p-1} u = 0 \tag{3.27}$$

is again closely related to the mean curvature flow problem (3.4). Namely, disregarding the higher-order term in h_x, (3.4) becomes

$$h_t = h_{xx} - \frac{1}{h}. \tag{3.28}$$

Putting $u = 1/h$ one finds

$$u_t = u_{xx} + u^3 - 2u_x^2/u, \tag{3.29}$$

which is (3.27) in one space dimension and $p = 3$, once more neglecting higher-order nonlinearities. As before, (3.27) has the exact blow-up solution

$$u = (p-1)^{\frac{1}{1-p}} t'^{-\frac{1}{p-1}}. \tag{3.30}$$

If $1 < p < p_c = \frac{d+2}{d-2}$, where d is the space dimension, then there are no other self-similar solutions to (3.27) [18], and blow-up is of the form (3.30) (see [118–120] for a recent review). As in the case of mean curvature flow, corrections to (3.30) are described by a slowly varying amplitude a:

$$u = t'^{1/(p-1)} (p-1)^{\frac{1}{1-p}} \left[1 - a H_2(\xi/2) + O(1/\tau^2)\right], \qquad \xi = x'/t'^{1/2}, \tag{3.31}$$

where a obeys the equation

$$a_\tau = -4pa^2. \tag{3.32}$$

This result holds in 1 space dimension. In higher dimensions, one has to replace x by the distance to the blow-up set.

This covers all ranges of exponents (larger than one, because otherwise there is no blow-up) in dimensions 1 and 2. The situation if $p > p_c$ is not so clear: if $p > 1 + \frac{2}{d}$ then there are solutions that blow-up and 'small' solutions that do not blow-up. Nevertheless, the

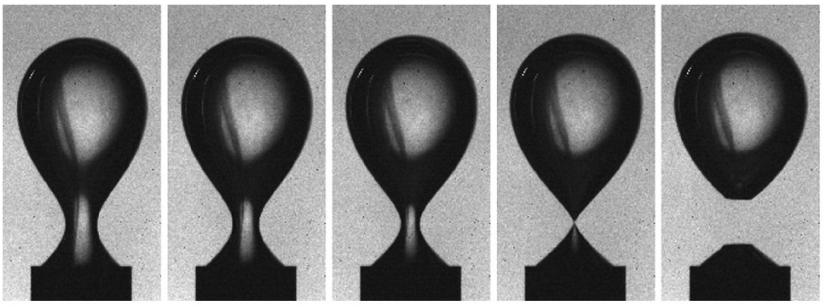

Figure 9. The pinch-off of an air bubble in water [125]. An initially smooth shape develops a localized pinch point. Reused with permission from [125]. Copyright 2007, American Institute of Physics.

construction of solutions as perturbations of constant self-similar solutions holds for any d and any $p > 1$. A simple generalization of (3.27) results from considering a nonlinear diffusion operator,

$$u_t - \nabla \cdot (|u|^m \nabla u) = u^p \tag{3.33}$$

and now the blow-up character depends on the two parameters m and p, see [121].

3.2. Cubic nonlinearity: cavity breakup and chemotaxis

More complex logarithmic corrections are possible if the linearization around the fixed point leads to a zero eigenvalue and cubic nonlinearities.

3.2.1. Cavity break-up. As shown in [122], the equation for a slender cavity or bubble is

$$\int_{-L}^{L} \frac{\ddot{a}(\xi, t)\, \mathrm{d}\xi}{\sqrt{(x-\xi)^2 + a(x,t)}} = \frac{\dot{a}^2}{2a}, \tag{3.34}$$

where $a(x,t) \equiv h^2(x,t)$ and $h(x,t)$ is the radius of the bubble. Dots denote derivatives with respect to time t. The length L measures the total size of the bubble. If for the moment one disregards boundary conditions and looks for solutions to (3.34) of cylindrical form, $a(x,t) = a_0(t)$, one can do the integral to find

$$\ddot{a}_0 \ln\left(\frac{4L^2}{a_0}\right) = \frac{\dot{a}_0^2}{2a_0}. \tag{3.35}$$

It is easy to show that an asymptotic solution of (3.35) is given by

$$a_0 \propto \frac{t'}{\tau^{1/2}}, \tag{3.36}$$

corresponding to a power law with a small logarithmic correction. Indeed, initial theories of bubble pinch-off [123, 124] treated the case of an approximately cylindrical cavity, which leads to the radial exponent $\alpha = 1/2$, with logarithmic corrections.

However both experiment [125] and simulation [122] show that the cylindrical solution is unstable; rather, the pinch region is rather localized, see figure 9. Therefore, it is not enough to treat the width of the cavity as a constant L; the width W is itself a time-dependent quantity. In [122] we show that to leading order the time evolution of the integral equation (3.34) can

be reduced to a set of ordinary differential equations for the minimum a_0 of $a(x,t)$, as well as its curvature a_0''.

Namely, the integral in (3.34) is dominated by a local contribution from the pinch region. To estimate this contribution, it is sufficient to expand the profile around the minimum at $z = 0$: $a(x,t) = a_0 + (a_0''/2)z^2 + O(z^4)$. As in previous theories, the integral depends logarithmically on a, but the axial length scale is provided by the inverse curvature $W \equiv (2a_0/a_0'')^{1/2}$. Thus evaluating (3.34) at the minimum, one obtains [122] to leading order

$$\ddot{a}_0 \ln(4W^2/a_0) = \dot{a}_0^2/(2a_0), \tag{3.37}$$

which is a coupled equation for a_0 and W. Thus, a second equation is needed to close the system, which is obtained by evaluating the second derivative of (3.34) at the pinch point:

$$\ddot{a}_0'' \ln\left(\frac{8}{e^3 a_0''}\right) - 2\frac{\ddot{a}_0 a_0''}{a_0} = \frac{\dot{a}_0 \dot{a}_0''}{a_0} - \frac{\dot{a}_0^2 a_0''}{2a_0^2}. \tag{3.38}$$

The two coupled equations (3.37) and (3.38) are most easily recast in terms of the time-dependent exponents

$$2\alpha \equiv -\partial_\tau a_0/a_0, \qquad 2\delta \equiv -\partial_\tau a_0''/a_0'', \tag{3.39}$$

where $\beta = \alpha - \delta$, so α, β are generalizations of the usual exponents in (1.2). The exponent δ characterizes the time dependence of the aspect ratio W. Returning to the collapse (3.35) predicted for a constant solution, one finds that $\alpha = 1/2$ and $\delta = 0$. In the spirit of the previous subsection, this is the fixed point corresponding to the cylindrical solution. Now we expand the values of α and δ around their expected asymptotic values $1/2$ and 0:

$$\alpha = 1/2 + u(\tau), \qquad \delta = v(\tau). \tag{3.40}$$

and put $w(\tau) = 1/\ln(a_0'')$.

To leading order, the resulting equations are

$$u_\tau = u + w/4, \qquad v_\tau = -v - w/4, \qquad w_\tau = 2vw^2. \tag{3.41}$$

The linearization around the fixed point thus has the eigenvalues 0 and -1, in addition to the eigenvalue 1 coming from time translation. As before, the vanishing eigenvalue is the origin of the slow approach to the fixed point observed for the present problem. The derivatives u_τ and v_τ are of lower order in the first two equations of (3.41), and thus to leading order $u = v$ and $v = -w/4$. Using this, the last equation of (3.41) can be simplified to

$$w_\tau = -w^3/2. \tag{3.42}$$

Equation (3.42) is analogous to (3.13), but has a degeneracy of third order, rather than second order. Equation (3.42) yields, in an expansion for small δ [122],

$$\alpha = 1/2 + \frac{1}{4\sqrt{\tau}} + O(\tau), \qquad \delta = \frac{1}{4\sqrt{\tau}} + O(\tau^{-3/2}). \tag{3.43}$$

Thus the exponents converge towards their asymptotic values $\alpha = \beta = 1/2$ only very slowly, as illustrated in figure 10. This explains why typical experimental values are found in the range $\alpha \approx 0.54$–0.58 [125], and why there is a weak dependence on initial conditions [126].

3.2.2. Keller–Segel model for chemotaxis. This model describes the aggregation of microorganisms driven by chemotactic stimuli. The problem has biological meaning in two space dimensions. If we describe the density of individuals by $u(x,t)$ and the concentration of the chemotactic agent by $v(x,t)$, then the Keller–Segel system reads

$$u_t = \Delta u - \chi \nabla \cdot (u \nabla v), \tag{3.44a}$$

$$\Gamma v_t = \Delta v + (u - 1), \tag{3.44b}$$

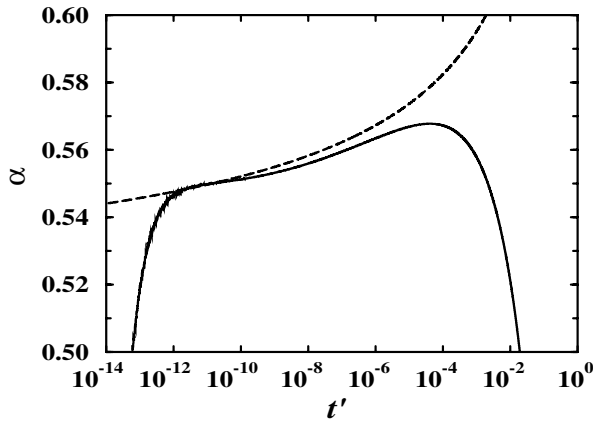

Figure 10. A comparison of the exponent α between full numerical simulations of bubble pinch-off (solid line) and the leading order asymptotic theory (3.43) (dashed line).

where Γ and χ are positive constants. In [13, 127] it was shown that for radially symmetric solutions of (3.44*a*) and (3.44*b*) singularities are such that to leading order u blows up in the form of a delta function. The profile close to the singularity is self-similar and of the form

$$u(r,t) = \frac{1}{R^2(t)} U\left(\frac{r}{R(t)}\right), \tag{3.45}$$

where

$$R(t) = C\mathrm{e}^{-\frac{1}{2}\tau - \frac{\sqrt{2}}{2}\tau^{\frac{1}{2}} - \frac{1}{4}\ln\tau + \frac{1}{4}\frac{\ln\tau}{\sqrt{\tau}}}(1 + o(1)) \tag{3.46}$$

and

$$U(\xi) = \frac{8}{\chi(1+\xi^2)}. \tag{3.47}$$

The result comes from a careful matched asymptotics analysis that, in our notation, amounts to introducing the time-dependent exponent

$$\gamma = -\partial_\tau R/R, \tag{3.48}$$

which has the fixed point $\gamma = 1/2$. Corrections are of the form

$$\gamma = \frac{1}{2} + \frac{\alpha}{2}\left(\alpha - \alpha^2 + 1\right), \tag{3.49}$$

where α is controlled by a third-order nonlinearity, as in the bubble problem:

$$\alpha_\tau = -\alpha^3(1 - \alpha + o(\alpha)). \tag{3.50}$$

3.3. Beyond all orders: the nonlinear Schrödinger equation

The cubic nonlinear Schrödinger equation

$$\mathrm{i}\varphi_t + \Delta\varphi + |\varphi|^2\varphi = 0 \tag{3.51}$$

appears in the description of beam focusing in a nonlinear optical medium, for which the space dimension is $d = 2$. Equation (3.51) belongs to the more general family of nonlinear Schrödinger equations of the form

$$\mathrm{i}\varphi_t + \Delta\varphi + |\varphi|^p\varphi = 0, \tag{3.52}$$

and in any dimension d. Of particular interest, from the point of view of singularities, is the *critical case* $p = 4/d$. In this case, singularities with slowly converging similarity exponents appear due to the presence of zero eigenvalues. We will describe this situation below, based on the formal construction of Zakharov [128], later proved rigorously by Galina Perelman [129]. At the moment, the explicit construction has only been given for $d = 1$, that is, for the quintic Schrödinger equation. The same blow-up estimates have been shown to hold for any space dimension $d < 6$ by Merle and Raphaël [130, 131], without making use of Zakharov's [128] formal construction. Merle and Raphaël also show that the stable solutions to be described below are in fact global attractors.

In the critical case (3.52) becomes in $d = 1$:

$$\mathrm{i}\varphi_t + \varphi_{xx} + |\varphi|^4 \varphi = 0. \tag{3.53}$$

This equation has explicit self-similar solutions (in the sense that rescaling $x \to \lambda x$, $t \to \lambda^2 t$, $\varphi \to \lambda^{\frac{1}{2}}\varphi$ leaves the solutions unchanged except for the trivial phase factor $\mathrm{e}^{-2\mathrm{i}\mu_0 \ln \lambda}$) of the form

$$\varphi(x,t) = \mathrm{e}^{\mathrm{i}\mu_0 \tau} \mathrm{e}^{-\frac{\xi^2}{8}\mathrm{i}} \frac{1}{t'^{\frac{1}{4}}} \varphi_0(\xi), \qquad \xi = x'/t'^{1/2}. \tag{3.54}$$

The function $\varphi_0(\xi)$ solves

$$-\varphi_{0,\xi\xi} + \varphi_0 - |\varphi_0|^4 \varphi_0 = 0, \tag{3.55}$$

and is given explicitly by

$$\varphi_0(\xi) = \frac{(3\mu_0)^{\frac{1}{4}}}{\cosh^{\frac{1}{2}}(2\sqrt{\mu_0}\xi)}. \tag{3.56}$$

We seek solutions of (3.53) using a generalization of (3.54), which allow for a variation of the phase factors, and the amplitude to be different from a power law:

$$\varphi(x,t) = \mathrm{e}^{\mathrm{i}\mu(t) - \mathrm{i}\beta(t)z^2/4} \lambda^{\frac{1}{2}}(t) \varphi_a(z), \tag{3.57}$$

where $z = \lambda(t)x$ and φ_a satisfies

$$-\varphi_{a,\xi\xi} + \varphi_a - \tfrac{1}{4} a z^2 \varphi_a - |\varphi_a|^4 \varphi_a = 0. \tag{3.58}$$

When $h\ (= \sqrt{a})$ is constant, (3.57) is a solution of (3.53) if (μ, λ, β) satisfy

$$\mu_t = \lambda^2, \tag{3.59a}$$

$$\lambda^{-3}\lambda_t = \beta, \tag{3.59b}$$

$$\beta_t + \lambda^2 \beta^2 = \lambda^2 h^2. \tag{3.59c}$$

Note that the equation for μ is uncoupled, so we only need to solve the equations for (λ, β) simultaneously and then integrate the equation for μ. It is interesting for the following that, in addition to the solutions for constant a, one can let a vary slowly in time. The resulting system for (λ, β, h) is

$$\lambda^{-3}\lambda_t = \beta, \tag{3.60a}$$

$$\beta_t + \lambda^2 \beta^2 = \lambda^2 h^2, \tag{3.60b}$$

$$h_t = -c\lambda^2 \mathrm{e}^{-S_0/h}/h. \tag{3.60c}$$

Note the appearance of the factor $\mathrm{e}^{-S_0/h}$ in the last equation, which comes from a semiclassical limit of a linear Schrödinger equation with appropriate potential (see [129]), and

$$S_0 = \int_0^2 \sqrt{1 - s^2/4}\, \mathrm{d}s = \frac{\pi}{2}. \tag{3.61}$$

It follows from the presence of this factor that the nonlinearity is beyond all orders, smaller than any given power, in contrast to the examples given above.

As in section 3.2.1, we rewrite the equations in terms of similarity exponents,

$$\alpha = -\frac{\lambda_\tau}{\lambda}, \qquad \gamma = -\frac{\beta_\tau}{\beta}, \qquad \delta = -\frac{h_\tau}{h} \tag{3.62}$$

to obtain the system:

$$\alpha_\tau = -(1 + 2\alpha + \gamma)\alpha, \tag{3.63a}$$

$$\gamma_\tau = (1 + 2\alpha + \gamma)\alpha - (\gamma + \alpha)(1 + 2\alpha + 2\delta - \gamma), \tag{3.63b}$$

$$\delta_\tau = (-1 - 2\alpha + 2\delta)\delta - \delta^2 \frac{S_0}{h}, \tag{3.63c}$$

$$h_\tau = -\delta h. \tag{3.63d}$$

The advantage of this formulation is that the exponents have fixed points. There are two families of equilibrium points for (3.63*a*)–(3.63*d*):

(1) $\alpha = -\frac{1}{2}$, $\gamma = 0$, $\delta = 0$, h arbitrary positive or zero.
(2) $\alpha = -1$, $\gamma = 1$, $\delta = 0$, h arbitrary positive or zero.

We first investigate case (1) by writing

$$\alpha = -\tfrac{1}{2} + \alpha_1, \qquad \gamma = \gamma_1, \qquad \delta = \delta_1, \qquad h = h_1. \tag{3.64}$$

The final fixed point corresponding to the singularity is going to be $\alpha_1 = \gamma_1 = \delta_1 = h_1 = 0$. However, there are also equilibrium points for *any* $h > 0$, in which case the linearization reads

$$\alpha_{1,\tau} = \alpha_1 + \tfrac{1}{2}\gamma_1, \tag{3.65a}$$

$$\gamma_{1,\tau} = -\gamma_1 + \delta_1, \tag{3.65b}$$

$$\delta_{1,\tau} = 2\delta_1^2 - 2\alpha_1\delta_1 - \delta_1^2 \frac{S_0}{h}. \tag{3.65c}$$

This system has the matrix

$$A = \begin{pmatrix} 1 & \frac{1}{2} & 0 \\ 0 & -1 & 1 \\ 0 & 0 & 0 \end{pmatrix},$$

whose eigenvalues are 1, 0 and -1. The vanishing eigenvalue corresponds to the line of equilibrium points for $h > 0$, the positive eigenvalue to the direction of instability generated by a change in blow-up time. The eigenvector corresponding to the negative eigenvalue gives the direction of the stable manifold.

At the point $h = 0$, there is an additional vanishing eigenvalue, and the equations become

$$\alpha_{1,\tau'} = (\alpha_1 + \tfrac{1}{2}\gamma_1)h_1, \tag{3.66a}$$

$$\gamma_{1,\tau'} = (-\gamma_1 + \delta_1)h_1, \tag{3.66b}$$

$$\delta_{1,\tau'} = (2\delta_1^2 - 2\alpha_1\delta_1)h_1 - \delta_1^2 S_0, \tag{3.66c}$$

$$h_{1,\tau'} = -\delta_1 h_1^2, \tag{3.66d}$$

where $\mathrm{d}\tau' = \mathrm{d}\tau/h_1$. The first two equations reduce to leading order to $\gamma_1 = \delta_1 h_1$ and $\alpha_1 = -\delta_1 h_1^2/2$, while the last two equations reduce to the nonlinear system:

$$\delta_{1,\tau'} = -\delta_1^2 S_0, \qquad h_{1,\tau'} = -\delta_1 h_1^2, \qquad \tau_{\tau'} = h_1. \tag{3.67}$$

In the original τ-variable, the dynamical system is

$$\delta_{1,\tau} = -\delta_1^2 S_0/h_1 \quad h_{1,\tau'} = -\delta_1 h_1, \tag{3.68}$$

which controls the approach to the fixed point. System (3.68) is two-dimensional, corresponding to the two vanishing eigenvalues.

Integrating the first equation of (3.67) one gets $\delta_1 \sim 1/(S_0\tau')$, and thus form the second equation $h_1 \sim S_0/\ln\tau'$. From the last equation one obtains to leading order $\tau' \sim \tau\ln\tau/S_0$, so that

$$h_1 \sim \frac{S_0}{\ln\tau}, \qquad \delta_1 \sim \frac{1}{\tau\ln\tau}. \tag{3.69}$$

Thus we can conclude that

$$\alpha(\tau) \simeq \frac{1}{2} - \frac{1}{2\tau\ln\tau}, \qquad \gamma(\tau) \simeq \frac{1}{\tau\ln\tau}, \qquad \delta(\tau) \simeq \frac{1}{\tau\ln\tau}. \tag{3.70}$$

In this fashion, one can construct a singular solution such that

$$\varphi(x,t) = \mathrm{e}^{-\mathrm{i}\tau\ln\tau - \mathrm{i}\frac{1}{t'}x^2/4}\frac{(\ln\tau)^{\frac{1}{4}}}{t'^{\frac{1}{4}}}\varphi_{h^2\tau}\left(\frac{(\ln\tau)^{\frac{1}{2}}}{t'^{\frac{1}{2}}}x\right)$$

$$\sim \mathrm{e}^{-\mathrm{i}\tau\ln\tau}\frac{(\ln\tau)^{\frac{1}{4}}}{t'^{\frac{1}{4}}}\varphi_0\left(\frac{(\ln\tau)^{\frac{1}{2}}}{t'^{\frac{1}{2}}}x\right). \tag{3.71}$$

Note the remarkable smallness of this correction to the 'natural' scaling exponent of $t'^{1/4}$, which enters only as the logarithm of logarithmic time τ.

The fixed points (2) can be analysed in a similar fashion. The linearization leads to

$$\alpha_{1,\tau} = 2\alpha_1 + \gamma_1, \tag{3.72a}$$

$$\gamma_{1,\tau} = \gamma_1, \tag{3.72b}$$

$$\delta_{1,\tau} = \delta_1. \tag{3.72c}$$

All eigenvalues are positive, so one cannot expect these equilibrium points to be stable.

One may also consider the blow-up of vortex solutions to both critical and supercritical solutions to nonlinear Schrödinger equation in 2D. These are a subset of the general solutions to NLSE that present a phase singularity at a given point. The singularities appear in the form of collapse of rings at that point. Both the existence of such solutions and their stability have been considered recently in [132, 133].

3.3.1. Other nonlinear dispersive equations. The nonlinear Schrödinger equation belongs to the broader class of nonlinear dispersive equations, for which many questions concerning existence and qualitative properties of singular solutions are still open. Nevertheless, there have been recent developments that we describe next.

The Korteweg–de Vries (KdV) equation

$$u_t + (u_{xx} + u^2)_x = 0 \tag{3.73}$$

describes the propagation of waves with large wavelength in a dispersive medium. For example, this is the case of water waves in the shallow-water approximation, where u represents the height of the wave. In the case of an arbitrary exponent of the nonlinearity, (3.73) becomes the generalized Korteweg–de Vries equation:

$$u_t + (u_{xx} + u^p)_x = 0, \qquad p > 1. \tag{3.74}$$

Based on numerical simulations, [134] conjectured the existence of singular solutions of (3.74) with type-I self-similarity if $p \geqslant 5$. In [135, 136] it was shown that in the *critical case* $p = 5$ solutions may blow-up both in finite and in infinite time. Lower bounds on the blow-up rate were obtained, but they exclude blow-up in the self-similar manner proposed by [134].

The Camassa–Holm equation

$$u_t - u_{xxt} + 3u_x u = 2u_x u_{xx} + u_{xxx} u \tag{3.75}$$

also represents unidirectional propagation of surface waves on a shallow layer of water. Its main advantage with respect to KdV is the existence of singularities representing breaking waves [137]. The structure of these singularities in terms of similarity variables has not been addressed to our knowledge.

4. Travelling wave

The pinching of a liquid thread in the presence of an external fluid is described by the Stokes equation [138]. For simplicity, we consider the case that the viscosity η of the fluid in the drop and that of the external fluid are the same. An experimental photograph of this situation is shown in figure 1. To further simplify the problem, we make the assumption (the full problem is completely analogous) that the fluid thread is slender. Then the equations given in [5] simplify to

$$h_t = -v_x h/2 - v h_x, \tag{4.1}$$

where

$$v = \frac{1}{4} \int_{x_-}^{x_+} \left(\frac{h^2(y)}{\sqrt{h^2(y) + (x-y)^2}} \right)_y \kappa \, \mathrm{d}y, \tag{4.2}$$

and the mean curvature is given by (2.2). Here we have written the velocity in units of the capillary speed $v_\eta = \gamma/\eta$. The limits of integration x_- and x_+ are, for example, the positions of the plates which hold a liquid bridge [139].

Dimensionally, one would once more expect a local solution of the form

$$h(x,t) = t' H\left(\frac{x'}{t'}\right), \tag{4.3}$$

and $H(\xi)$ has to be a linear function at infinity to match to a time-independent outer solution. In similarity variables, (4.2) has the form

$$V(\xi) = \frac{1}{4} \int_{-x_b/t'}^{x_{b/t'}} \left(\frac{H^2(\eta)}{\sqrt{H^2(\eta) + (\xi-\eta)^2}}) \right)_\eta \kappa \, \mathrm{d}\eta. \tag{4.4}$$

We have chosen x_b as a real-space variable close to the pinch point, such that the similarity description is valid in $[-x_b, x_b]$. But if H is linear, the integral in (4.4) diverges like $b \ln t'$, where

$$b = -\frac{1}{4} \left[\frac{H_+}{1+H_+^2} + \frac{H_-}{1+H_-^2} \right]. \tag{4.5}$$

Here H_+ and H_- are the slopes of the similarity profile at $\pm\infty$. But this means that a simple 'fixed point' solution (4.3) is impossible.

However by subtracting the singularity as $t' \to 0$, one can define a self-similar velocity profile according to

$$V^{(\mathrm{fin})}(\xi) = \lim_{\Lambda\to\infty} \frac{1}{4} \int_{-\Lambda}^{\Lambda} \left(\frac{H^2(\eta)}{\sqrt{H^2(\eta) + (\xi-\eta)^2}} \right)_\eta \kappa \, \mathrm{d}\eta + b \ln \Lambda, \tag{4.6}$$

where now

$$V(\xi) = V^{(\mathrm{fin})}(\xi) - b\tau, \tag{4.7}$$

and an arbitrary constant has been absorbed into $V^{(\mathrm{fin})}$. In terms of $V^{(\mathrm{fin})}$, and putting

$$h(x,t) = t' H(\xi,\tau), \tag{4.8}$$

the dynamical system for H becomes

$$H_\tau = H - \left(\xi + V^{(\mathrm{fin})}\right) H_\xi - H V_\xi^{(\mathrm{fin})}/2 + b\tau H_\xi. \tag{4.9}$$

This equation has a solution in the form of a travelling wave:

$$H(\xi,\tau) = \overline{H}(\zeta), \quad V^{(\mathrm{fin})}(\xi,\tau) = \overline{V}(\zeta), \qquad \text{where} \quad \zeta = \xi - b\tau. \tag{4.10}$$

The profiles $\overline{H}$, $\overline{V}$ of the travelling wave obey the equation

$$\overline{H} - (\zeta + \overline{V})\overline{H}_\zeta = \overline{H}\,\overline{V}_\zeta/2. \tag{4.11}$$

The numerical solution of the integro-differential equation (4.11) gives

$$h_{\min} = a_{\mathrm{out}} v_\eta t', \qquad \text{where} \quad a_{\mathrm{out}} = 0.033. \tag{4.12}$$

The slopes of the solution away from the pinch point are given by

$$H_+ = 6.6 \qquad \text{and} \qquad H_- = -0.074, \tag{4.13}$$

which means the solution is very asymmetric, as confirmed directly from figure 1. These results are reasonably close to the exact result, based on a full solution of the Stokes equation [5]; in particular, the normalized minimum radius is $a_{\mathrm{out}} = 0.0335$ for the full problem.

5. Limit cycles

An example for this kind of blow-up was introduced into the literature in [15] in the context of cosmology. There is considerable numerical evidence [140] that discrete self-similarity occurs at the mass threshold for the formation of a black hole. The same type of self-similarity has also been proposed for singularities of the Euler equation [67, 141], the porous medium equation driven by buoyancy [141], and for a variety of other phenomena [142]. A reformulation of the original cosmological problem leads to the following system:

$$f_x = \frac{(a^2-1)f}{x}, \tag{5.1a}$$

$$(a^{-2})_x = \frac{1-(1+U^2+V^2)/a^2}{x}, \tag{5.1b}$$

$$(a^{-2})_t = \left[\frac{(f+x)U^2 - (f-x)V^2}{x} + 1\right]/a^2 - 1, \tag{5.1c}$$

$$U_x = \frac{f[(1-a^2)U+V] - xU_t}{x(f+x)}, \tag{5.1d}$$

$$V_x = \frac{f[(1-a^2)U+V] + xV_t}{x(f-x)}. \tag{5.1e}$$

In [16], the self-similar description corresponding to system (5.1*a*)–(5.1*e*) was solved using formal asymptotics and numerical shooting procedures. This leads to the solutions observed in [15]. We now propose another system, which shares some of the structure of (5.1*a*)–(5.1*e*), but which we are able to solve analytically:

$$u_t(x,t) = 2f(x,t)v(x,t), \tag{5.2a}$$

$$v_t(x,t) = -2f(x,t)u(x,t), \tag{5.2b}$$

$$f_t(x,t) = f^2(x,t). \tag{5.2c}$$

System (5.2*a*)–(5.2*c*) is driven by the simplest type of blow-up equation (5.2*c*), and can be solved using characteristics. However, in the spirit of this review, we transform to similarity variables according to

$$u = U(\xi, \tau), \tag{5.3a}$$

$$v = V(\xi, \tau), \tag{5.3b}$$

$$f = t'^{-1} F(\xi, \tau). \tag{5.3c}$$

It is seen directly from (5.2*c*) that f first blows up at a local maximum $f_{\max} > 0$. Near a maximum, the horizontal scale is the square root of the vertical scale t', and thus we must have $\xi = x'/t'^{1/2}$. With that, the similarity equations become

$$U_\tau = -\xi U_\xi/2 + FV, \tag{5.4a}$$

$$V_\tau = -\xi V_\xi/2 - FU, \tag{5.4b}$$

$$F_\tau = -F - \xi F_\xi/2 + F^2. \tag{5.4c}$$

The fixed point solution of the last equation is

$$F = \frac{1}{1 + c\xi^2}, \tag{5.5}$$

where $c > 0$ is a constant. The equations for U, V are solved by the ansatz

$$U = U_0 \sin\left(C(\xi) + \tau\right), \qquad V = U_0 \cos\left(C(\xi) + \tau\right), \tag{5.6}$$

and for the function $C(\xi)$ one finds

$$\xi C'(\xi)/2 = F - 1, \tag{5.7}$$

with solution $C(\xi) = -\ln(1 + c\xi^2)$. Thus (a single component of) the singular solution is indeed of the general form

$$U = \psi(\phi(\xi) + \tau), \tag{5.8}$$

where ψ is *periodic* in τ. This is a particularly simple version of discretely self-similar behaviour, i.e. when T is the period of ψ, the same self-similar picture is obtained for $\tau = \tau_0 + nT$.

6. Strange attractors and exotic behaviour

In connection with limit cycles and in the context of singularities in relativity, a few interesting situations have been found numerically quite recently. One of them is the existence of Hopf bifurcations where a self-similar solution (a stable fixed point) is transformed into a discrete self-similar solution (limit cycle) as a certain parameter varies (see [143]). Other kinds of bifurcations, for example of the Shilnikov type, are found as well [144]. Before coming to simple explicit examples, we mention that possible complex dynamics in τ has long been suggested for simplified versions of the inviscid Euler equations [141, 145, 146]. For a critical discussion of this work, see [81, 147].

The problems considered in these papers were the 2D axisymmetric Euler equations with swirl, which produces a centripetal force. In the limit that the rotation is confined to a small annulus, the direction of acceleration is locally uniform, and the equation reduces to that of 2D Boussinesq convection, where the centripetal force is replaced by a 'gravity' force. Another related model is 2D porous medium convection, for which the equation reads

$$\frac{\partial T}{\partial t} + \left(T\boldsymbol{e}_y - \nabla\phi\right) \cdot \nabla T = 0, \tag{6.1}$$

where $\boldsymbol{v} = T\boldsymbol{e}_y - \nabla\phi$ plays the role of the velocity field and T is the temperature. The potential ϕ follows from the constraint of incompressibility, which gives $\triangle\phi = T_y$. Simulations provide evidence of a self-similar dynamics of the form [141]

$$T = t'^{\eta} M(\boldsymbol{x}'/t'^{1+\eta}, \tau), \tag{6.2}$$

where η is approximately 0.1 and M is a function that is slowly varying with τ.

Depending on the model, both periodic behaviour as well as more complicated, chaotic motion has been observed in numerical simulations. Oscillations of temperature in τ are motivated by the observation that a sharp, curved interface (i.e. the transition region between a rising 'bubble' of hot fluid and its surroundings) becomes unstable and rolls up. However, owing to incompressibility, the sheet is also stretched, which stabilizes the interface, leading to an eventual decrease in gradients. Locality suggests that this process could repeat itself periodically on smaller and smaller scales [141]. However, simulations of the Euler equation have also shown examples of a more complicated dependence on τ, which might be chaotic behaviour [145]. We also mention that corresponding chaotic behaviour has been proposed for the description of spin glasses in the theory of critical phenomena [148]. We now give some explicit examples of chaos in the description of a singularity.

In section 3.1.1 we treated a system of an infinite number of ordinary differential equations for the coefficients of the expansion of an arbitrary perturbation to an explicit solution. Such high-dimensional systems in principle allow for a rich variety of dynamical behaviour, including that found in classical finite dimensional dynamical systems, such as chaos. Consider, for instance, an equation for the perturbation g (the analogue of (3.7)) of the form

$$g_\tau = Lg + F(g, g), \tag{6.3}$$

where Lg is a linear operator. Assuming an appropriate nonlinear structure for the function F, an arbitrary nonlinear (chaotic) dynamics can be added.

To give an explicit example of a system of PDEs exhibiting chaotic dynamics, consider the structure of the example given in section 5. It can be generalized to produce *any* low-dimensional dynamics near the singularity, as follows by considering system (5.2*a*)–(5.2*c*)

$$u_t^{(i)}(x,t) = 2f F_i(\{u^{(i)}\}), \qquad i = 1, \ldots, n, \tag{6.4a}$$

$$f_t(x,t) = f^2(x,t). \tag{6.4b}$$

Using the ansatz analogous to (5.6):

$$u^{(i)} = U^{(i)}\left(C(\xi) + \tau, \xi\right), \tag{6.5}$$

and choosing $C(\xi) = -\ln(1 + c\xi^2)$, one obtains the system

$$U_\tau^{(i)} = F_i\left\{U^{(i)}\right\}. \tag{6.6}$$

To be specific, we consider $n = 3$ and

$$F_1 = \sigma(u^{(2)} - u^{(1)}), \qquad F_2 = \rho u^{(1)} - u^{(2)} - u^{(1)}u^{(3)}, \qquad F_3 = u^{(1)}u^{(2)} - \beta u^{(3)}, \tag{6.7}$$

so that (6.6) becomes the Lorenz system [149]. As before, for $t' \to 0$, the variable τ goes to infinity, and near the singularity one is exploring the long-time behaviour of the dynamical system (6.5). In the case of (6.7), and for sufficiently large ρ, the resulting dynamics will be chaotic. Specifically, taking $\sigma = 10$, $\rho = 28$ and $\beta = 8/3$, as done by Lorenz [150], the maximal Lyapunov exponent is 0.906. The initial conditions with which (6.5) is to be solved depend on ξ. Thus the chaotic dynamics will follow a completely different trajectory for each space point. As a result, it will be very difficult to detect self-similar behaviour of this type as such, even if data arbitrarily close to the singularity time are taken. If, for example, a rescaled

spatial picture is observed at constant intervals of logarithmic time τ, the spatial structure of the singularity will appear to be very different. However, as pointed out in [145], chaotic motion is characterized by unstable periodic orbits, for which one could search numerically.

7. Multiple singularities

The singularities described so far occur at a single point x_0 at a given time t_0. This need not be the case, but blow-up may instead occur on sets of varying complexity, including sets of finite measure. We begin with a case where singularity formation involves two different points in space.

7.1. Hele–Shaw equation

A particularly rich singularity structure is found for a special case of (2.7) in one space dimension with $n = 1$. Dropping the second term on the right, which will typically be small, one arrives at

$$h_t + (hh_{xxx})_x = 0. \tag{7.1}$$

This is a simplified model for a neck of liquid of width h confined between two parallel plates, a so-called Hele–Shaw cell. which is a simplified model for the free surface in a so-called Hele–Shaw cell [151]. Breakup of a fluid neck inside the cell corresponds to h going to zero in finite time.

Singular solutions displaying type-I self-similarity would be of the form

$$h(x,t) = t'^{\alpha} H(x'/t'^{(\alpha+1)/4}), \tag{7.2}$$

but are never observed. Instead, several types of pinch solutions different from (7.2) have been found for (7.1) using a combination of numerics and asymptotic arguments [102, 152, 153]. On the one hand, singularities exhibit type-II self-similarity. On the other hand, the simple structure (7.2) is broken by the fact that the location of the pinch point is *moving* in space. The root for this behaviour lies in the fact that two singularities are *interacting* over a distance much larger than their own spatial extent. Below we report on three different kinds of singularities whose existence has been confirmed by numerical simulation of (7.1).

The first kind of singularity was called the *imploding singularity* in [153], since it consists of two self-similar solutions which form mirror images, and which collide at the singular time. Locally, the solution can be written

$$h(x,t) = t'^{6} H((x' + at')/t'^{3}), \tag{7.3}$$

where $-a$ is the constant speed of the singular point. Note that the scaling exponents do not agree with (7.2). The reason is that the singularity is moving, so h is the solution of

$$hh_{xxx} = J(t') \equiv t'^{3}, \tag{7.4}$$

where J is determined by matching to an outer region. The similarity profile H is a solution of the equation $HH''' = 1$, with boundary conditions

$$H(\eta) \propto \eta^2/2, \ \eta \to -\infty; \qquad H(\eta) \propto \sqrt{8/3}(A - \eta)^{3/2}, \qquad \eta \to \infty. \tag{7.5}$$

One might wonder whether this behaviour is generic, in the sense that it might depend on the initial conditions being exactly symmetric around the eventual point of blow up. The simulation of (7.1) shown in figure 11 shows that this is *not* the case. The initial condition is

$$h(x,0) = 1 - (1 - w)\left[\tfrac{3}{2}\cos \pi x - \tfrac{6}{10}\cos 2\pi x + \tfrac{1}{10}\cos 3\pi x(1 + \delta \sin 2\pi x)\right], \tag{7.6}$$

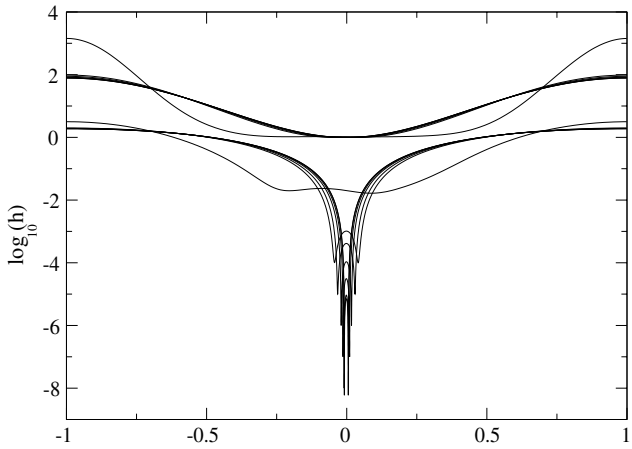

Figure 11. A simulation of (7.1) with spatially periodic boundary conditions and initial condition (7.6), with $w = 0.02$ and $\delta = 0.1$.

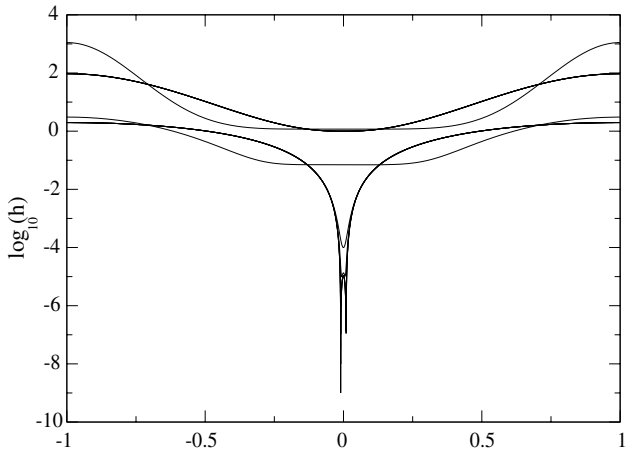

Figure 12. Same as figure 11, but parameters $w = 0.07$ and $\delta = 0.01$.

which for $\delta = 0$ reduces to the symmetric initial condition considered by [153]. The type of singularity that is observed (or no singularity at all) depends on the parameter w. The simulation shown in figure 11 shows that even at finite δ (non-symmetric initial conditions) the final collapse is described by a symmetric solution.

The second kind is the *exploding singularity* [153], since now the two self-similar solutions are moving apart, cf figure 12. This time even a very small asymmetry ($\delta = 1/100$) makes one pinching event 'win' over the other. However, this does not affect the asymptotics described briefly below. Locally, the solution can be written

$$h(x,t) = \delta^2(t')H((x' - at')/\delta(t')), \tag{7.7}$$

with $\delta = t'/\ln(t')$, which is similar to examples considered in section 3. However, an additional complication consists of the fact that the singularity is moving, so there is a coupling to the parabolic region between the two pinch points. This matching is unaffected by the fact that in the simulation shown in figure 12 one side of the solution touches down first. In [153], a

possible generalization is also conjectured, which has the form

$$h(x,t) = \delta^2(t')H((x' - at'^{\frac{r-1}{2}})/\delta(t')), \tag{7.8}$$

and $\delta = t'^{\frac{r-1}{2}}/\ln t'$. In principle, any value of r is possible, but numerical evidence has been found for $r \approx 3$ (above) and $r \approx 5/2$ only.

Finally, a third type is the *symmetric singularity* of [153], which does not move. In that case, the structure of the solution is

$$h(x,t) = h_0(t')H((x'/\delta(t')), \tag{7.9}$$

with $h_0 = \delta^2 P(\ln \delta)$, where P is a polynomial. The time dependence of δ is not reported. Evidently, many aspects of the exploding and of the symmetric singularity remain to be confirmed and/or to be worked out in more detail.

The most intriguing feature of the Hele–Shaw equation (7.1) is that several types of *stable* singularities have been observed for the same equation. Within a one-parameter family of smooth initial conditions, all three types of singularities can be realized as $h \to 0$. Each type is observed over an interval of the parameter w. Near the boundary of the intervals, a very interesting crossover phenomenon occurs: the solution is seen to follow one type of singularity at first (the exploding singularity, say), and then crosses over to a solution of another singularity (the imploding singularity). The dynamics of each singularity can be followed numerically over many decades in t'. By tuning w, the crossover can be made to occur at arbitrarily small values of h.

The switch in behaviour is driven by the slow dynamics of scaling regions exterior to (7.3) or (7.7). It is a signature of the very long-ranged interactions (both in real space as well as in scale), which exist in (7.1). Thus an outside development can trigger a change of behaviour that is taking place on the local scale of the singularity. To mention another example, applying different boundary conditions for the pressure at the outside of the cell can change the singular behaviour completely [154]. This makes the crossover behaviour of (7.1) very different from that observed for drop pinch-off (cf (2.10) and (2.11)), which is driven by a change in the dominant balance between different terms in (2.11).

7.2. Semilinear wave equation

It appears that the Hele–Shaw equation is not an isolated example, but rather is representative of a more general phenomenon. Namely, another example of a potentially complex singularity structure is the semilinear wave equation

$$u_{tt} - \Delta u = |u|^{p-1}u, \qquad p > 1. \tag{7.10}$$

It has trivial singular solutions of the form

$$u(x,t) = b_0(T-t)^{-\frac{2}{p-1}}, \tag{7.11}$$

with $b_0 = [\frac{2(p+1)}{(p-1)^2}]^{\frac{1}{p-1}}$. Nevertheless, the existence of different self-similar solutions is known in a few particular cases, such as the case $p \geqslant 7$, where p is an odd integer (see [155]) or in space dimension $d = 1$ (see [156]).

The character of the blow-up is controlled by the blow-up curve $T(x)$, which is the locus where the equation first blows up at a given point in space. It has been shown for $d = 1$ [157] that there exists a set of *characteristic* points, where the blow-up curve locally coincides with the characteristics of (7.10). The set of non-characteristic points I_0 is open, and T is C^1 on I_0. Recently, it has been shown [158] that the blow-up at characteristic points is of type II. Even more intriguingly, it appears [158] that the structure of blow-up at these points is such that the singularity results from the *collision* of two peaks at the blow-up point, very similar to the observation shown in figure 11.

7.3. More complicated sets

In the Hele–Shaw equation of the previous subsection, different parts of the solution, characterized by different scaling laws, interacted with each other. In the generic case, however, finally blow-up only occurred at a single point in space. An example where singularities may even occur on sets of finite measure is given by reaction–diffusion equations of the family

$$u_t - \Delta u = u^p - b\,|\nabla u|^q \qquad \text{for} \quad x \in \Omega. \tag{7.12}$$

where Ω is any bounded, open set in dimension d. Depending on the values of $p > 1$ and $q > 1$ singularities of (7.12) may be regional (u blows up in subsets of Ω of finite measure) or even global (the solution blows up in the whole domain); see for instance [159] and references therein.

Singularities may even happen in sets of fractional Hausdorff dimension, i.e. fractals. This is the case of the inviscid one-dimensional system for jet breakup (cf [160]) and might be case of the Navier–Stokes system in three dimensions, where the dimension of the singular set at the time of first blow-up is at most 1 (cf [161]). This connects to the second issue we did not address here. It is the nature of the singular sets both in space and time, i.e. including possible continuation of solutions after the singularity. In some instances, existence of global in time (for all $0 \leqslant t < \infty$) solutions to nonlinear problems can be established in a *weak sense*. For example, this has been achieved for systems such as the Navier–Stokes equations [162], reaction–diffusion equations [163], and hyperbolic systems of conservation laws [96]. Weak solutions allow for singularities to develop both in space and time. In the case of the three-dimensional Navier–Stokes system, the impossibility of singularities 'moving' in time, that is of curves $\boldsymbol{x} = \boldsymbol{\varphi}(t)$ within the singular set is well known [161]. Hence, provided certain kinds of singularities do not persist in time, the question is how to continue the solutions after a singularity has developed.

Acknowledgments

A first version of this paper was an outgrowth of discussions between the authors and R Deegan, preparing a workshop on singularities at the Isaac Newton Institute, Cambridge. The present version was written during the programme: 'Singularities in mechanics: formation, propagation and microscopic description', organized with C Josserand and L Saint-Raymond, which took place between January and April 2008 at the Institut Henri Poincaré in Paris. We are grateful to all participants for their input, in particular C Bardos, M Brenner, M Escobedo, F Merle, H K Moffatt, Y Pomeau, A Pumir, J Rauch, S Rica, L Vega, T Witten and S Wu. We also thank J M Martin-Garcia and J J L Velazquez for fruitful discussions and for providing us with valuable references.

References

[1] Levine H A 1990 *SIAM Rev.* **32** 262
[2] Caflisch R C and Papanicolau G (ed.) 1993 *Singularities in Fluids, Plasmas and Optics* (Dordrecht: Kluwer)
[3] Kadanoff L P 1997 *Phys. Today* **50** 11–12
[4] Straughan B 1998 *Explosive Instabilities in Mechanics* (Berlin: Springer)
[5] Cohen I, Brenner M P, Eggers J and Nagel S R 1999 *Phys. Rev. Lett.* **83** 1147
[6] Eggers J 1997 *Rev. Mod. Phys.* **69** 865–929
[7] Moffatt H K 2000 *J. Fluid Mech.* **409** 51
[8] Grauer R, Marliani C and Germaschewski K 1998 *Phys. Rev. Lett.* **80** 4177
[9] Córdoba D, Fontelos M A, Mancho A M and Rodrigo J L 2005 *PNAS* **102** 5949
[10] Audoly B and Boudaoud A 2003 *Phys. Rev. Lett.* **91** 086105

[11] Bergé L and Rasmussen J J 2002 *Phys. Lett.* A **304** 136
[12] Moll K D, Gaeta A L and Fibich G 2003 *Phys. Rev. Lett.* **90** 203902
[13] Herrero M A and Velázquez J J L 1996 *Math. Ann.* **306** 583–623
[14] Brenner M P, Constantin P, Kadanoff L P, Schenkel A and Venkataramani S C 1999 *Nonlinearity* **12** 1071
[15] Choptuik M W 1993 *Phys. Rev. Lett.* **70** 9
[16] Martin-Garcia J M and Gundlach C 2003 *Phys. Rev.* D **68** 024011
[17] Sornette D 2003 *Phys. Rep.* **378** 1–98
[18] Giga Y and Kohn R V 1985 *Commun. Pure Appl. Math.* **38** 297
[19] Giga Y and Kohn R V 1987 *Indiana Univ. Math. J.* **36** 1
[20] Galaktionov V A and Vazquez J L 2004 *A Stability Technique for Evolution Partial Differential Equations: A Dynamical Systems Approach* (Basle: Birkhauser)
[21] Coddington E A and Levinson N 1955 *Theory of Ordinary Dierential Equations* (New York: McGraw-Hill)
[22] Levitan B M and Sargsjan I S 1990 *Sturm–Liouville and Dirac Operators* (Berlin: Springer)
[23] Goldenfeld N 1993 *Lectures on Phase Transitions and the Renormalization Group* (Reading, MA: Addison-Wesley)
[24] Bricmont J, Kupiainen A and Lin G 1994 *Commun. Pure Appl. Math.* **47** 893
[25] Chen L, Debenedetti P G, Gear C W and Kevrekidis I G 2004 *J. Non-Newtonian Fluid Mech.* **120** 215
[26] Arnold V I 1984 *Catastrophe Theory* (Berlin: Springer)
[27] Pomeau Y, Le Berre M, Guyenne P and Grilli S 2008 *Nonlinearity* **21** T61–79
[28] Angenent S B and Aronson D G 2003 *J. Evol. Eqns* **3** 137
[29] Berry M V 2007 *Proc. R. Soc.* A **463** 3055
[30] Angenent S B and Velázquez J J L 1997 *J. Reine Angew. Math.* **482** 15
[31] Martin-Garcia J M and Gundlach C 2007 *Living Rev. Rel.* **10** 5 http://www.livingreviews.org/lrr-2007-5
[32] Barenblatt G I and Zel'dovich Y B 1972 *Ann. Rev. Fluid Mech.* **4** 285–312
[33] Sedov L I 1993 *Similarity and Dimensional Methods in Mechanics* (Boca Raton, FL: CRC Press)
[34] Sachdev P L 2004 *Shock Waves and Explosions* (London: Chapman and Hall)
[35] Barenblatt G I 1996 *Similarity Self-Similarity and Intermedeate Asymptotics* (Cambridge: Cambridge University Press)
[36] Mizushima I, Sato T, Taniguchi S and Tsunashima Y 2000 *Appl. Phys. Lett.* **77** 3290–2
[37] Nichols F A and Mullins W W 1965 *J. Appl. Phys.* **36** 1826
[38] Spohn H 1993 *J. Phys. I (France)* **3** 69
[39] Stone H A, Aziz M J and Margetis D 2005 *J. Appl. Phys.* **97** 113535
[40] Margetis D, Aziz M J and Stone H A 2004 *Phys. Rev.* B **69** 041404
[41] Margetis D, Fok P W, Aziz M J and Stone H A 2006 *Phys. Rev. Lett.* **97** 096102
[42] Eggers J 2005 *Z. Angew. Math. Mech.* **85** 400
[43] Bernoff A J, Bertozzi A L and Witelski T P 1998 *J. Stat. Phys.* **93** 725–76
[44] Pugh M C 2006 Notes on blowup and long wave unstable thin film equations and http://topo.math.auburn.edu/pub/2Olgas-proceedings/
[45] Zhang W W and Lister J R 1999 *Phys. Fluids* **11** 2454–62
[46] Witelski T P and Bernoff A J 2000 *Physica* D **147** 155–76
[47] Becker J and Grün G 2005 *J. Phys.: Condens. Matter* **17** S291–S307
[48] Chou K S and Kwong Y C 2007 *Nonlinearity* **20** 299–317
[49] Eggers J and Villermaux E 2008 *Rep. Prog. Phys.* **71** 036601
[50] Eggers J 1993 *Phys. Rev. Lett.* **71** 3458
[51] Brenner M P, Lister J R and Stone H A 1996 *Phys. Fluids* **8** 2827
[52] Papageorgiou D T 1995 *Phys. Fluids* **7** 1529
[53] Eggers J 2005 *Phys. Fluids* **17** 082106
[54] Doshi P, Cohen I, Zhang W W, Siegel M, Howell P, Basaran O A and Nagel S R 2003 *Science* **302** 1185
[55] Ting L and Keller J B 1990 *SIAM J. Appl. Math.* **50** 1533
[56] Fontelos M A and Velázquez J J L 1999 *SIAM J. Appl. Math.* **59** 2274
[57] Eggers J 2000 *SIAM J. Appl. Math.* **60** 1997
[58] Chen Y J and Steen P H 1997 *J. Fluid Mech.* **341** 245–267
[59] Day R F, Hinch E J and Lister J R 1998 *Phys. Rev. Lett.* **80** 704
[60] Leppinen D and Lister J 2003 *Phys. Fluids* **15** 568
[61] Lenard P 1887 *Ann. Phys. Chem.* **30** 209
[62] Vaynblat D, Lister J R and Witelski T P 2001 *Eur. J. Appl. Math.* **12** 209–232
[63] Gibbon J D, Moore D R and Stuart J T 2003 *Nonlinearity* **16** 1823
[64] Necas J, Ruzicka M and Sverak V 1996 *Acta Math.* **176** 283–94

[65] Pelz R B 1997 *Phys. Rev.* E **55** 1617–26
[66] Hou T Y and Li R 2008 *Physica* **237** 1937–44
[67] Pomeau Y and Sciamarella D 2005 *Physica* D **205** 215
[68] Goldstein S 1948 *Q. J. Mech. Appl. Math.* **1** 43–69
[69] Sychev V V, Ruban A I, Sychev V V and Korolev G L 1998 *Asymptotic Theory of Separated Flows* (Cambridge: Cambridge University Press)
[70] E W and Engquist B 1997 *Commun. Pure. Appl. Math.* **50** 1287–93
[71] Van Dommelen L L and Shen S F 1980 *J. Comput. Phys.* **38** 125–40
[72] Van Dommelen L L and Shen S F 1982 *Aspects of Aerodynamic Flows* ed T Cebeci (Berlin: Springer) pp 293–311
[73] Caflisch R E and Sammartino M 2000 *Z. Angew. Math. Mech.* **11–12** 733–44
[74] Elliott J W, Cowley S J and Smith F T 1983 *Geophys. Astrophys. Fluid Dyn.* **25** 77–138
[75] Cassel K W, Smith F T and Walker J D A 1996 *J. Fluid Mech.* **315** 223–56
[76] Saffman P G 1992 *Vortex Dynamics* (Cambridge: Cambridge University Press)
[77] Moore D W 1979 *Proc. R. Soc. Lond.* A **365** 105–19
[78] Caflisch R E and Orellana O F 1989 *SIAM J. Math. Anal.* **20** 293–307
[79] de la Hoz F, Fontelos M A and Vega L 2008 *J. Nonlin. Sci.* **18** 463–841
[80] Kambe T 1989 *Physica* D **37** 463
[81] Majda A J and Bertozzi A L 2002 *Vorticity and Incompressible Flow* (Cambridge: Cambridge University Press)
[82] Gutiérrez S, Rivas J and Vega L 2003 *Commun. Partial Diff. Eqns* **28** 927–68
[83] Craig W and Wayne C E 2007 *Russ. Math. Surv.* **62** 453–73
[84] Constantin P, Majda A and Tabak E 1994 *Nonlinearity* **7** 1495
[85] Chae D, Córdoba A, Córdoba D and Fontelos M A 2005 *Adv. Math.* **194** 203–23
[86] Córdoba A, Córdoba D and Fontelos M A 2005 *Ann. Math.* **162** 1377–89
[87] de la Hoz F and Fontelos M A 2008 *J. Phys. A: Math. Theor.* **41** 185204
[88] Moffatt H K 1963 *J. Fluid Mech.* **18** 1–18
[89] Carothers S D 1912 *Proc. R. Soc. Edinb.* **23** 292
[90] Sternberg E and Koiter W T 1958 *J. Appl. Mech.* **25** 575
[91] Batchelor G K 1967 *An Introduction to Fluid Dynamics* (Cambridge: Cambridge University Press)
[92] Solomentsev Y, Velegol D and Anderson J L 1997 *Phys. Fluids* **9** 1209
[93] Griffith W C and Bleakney W 1954 *Am. J. Phys.* **22** 597
[94] Alinhac S 1995 *Blowup for Nonlinear Hyperbolic Equations* (Basle: Birkhäuser)
[95] Whitham G B 1974 *Linear and Nonlinear Waves* (New York: Wiley)
[96] Dafermos C M 2005 *Grundlehren der Mathematischen Wissenschaften* vol 325 (Berlin: Springer)
[97] Bressan A 2000 *Hyperbolic Systems of Conservation Laws. The One Dimensional Cauchy Problem* (Oxford: Oxford University Press)
[98] Landau L D and Lifshitz E M 1984 *Fluid Mechanics* (Oxford: Pergamon)
[99] Rothert A, Richter R and Rehberg I 2003 *New J. Phys.* **5** 59
[100] Abramowitz M and Stegun I A 1968 *Handbook of Mathematical Functions* (NewYork: Dover)
[101] Burton J C and Taborek P 2007 *Phys. Fluids* **19** 102109
[102] Dupont T F, Goldstein R E, Kadanoff L P and Zhou S 1993 *Phys. Rev.* E **47** 4182
[103] Barenblatt G I 2003 *Scaling* (Cambridge: Cambridge University Press)
[104] Guderley G 1942 *Luftfahrtforschung* **19** 302
[105] Brenner M P and Witelski T P 1998 *J. Stat. Phys.* **93** 863
[106] Chavanis P H and Sire C 2004 *Phys. Rev.* E **69** 016116
[107] Lacaze R, Lallemand P, Pomeau Y and Rica S 2001 *Physica* D **152** 779
[108] Josserand C, Pomeau Y and Rica S 2006 *J. Low Temp. Phys.* **145** 231
[109] Filippas S and Kohn R V 1992 *Commun. Pure Appl. Math.* **45** 821–69
[110] Velázquez J J L, Galaktionov V A and Herrero M A 1991 *Comput. Math. Math. Phys.* **31** 46–55
[111] Ishiguro R, Graner F, Rolley E, Balibar S and Eggers J 2007 *Phys. Rev.* E **75** 041606
[112] Ishiguro R, Graner F, Rolley E and Balibar S 2004 *Phys. Rev. Lett.* **93** 235301
[113] Altschuler S, Angenent S and Giga Y 1995 *J. Geom. Anal.* **5** 293
[114] Huisken G 1993 *Proc. Symp. Pure Math.* **54** 175–91
[115] Hamilton R S 1982 *J. Diff. Geom.* **17** 255–306
[116] Perelman G 2003 Ricci flow with surgery on three-manifolds and http://arxiv.org/abs/math.DG/0303109
[117] Angenent S and Knopf D 2007 *Commun. Anal. Geom.* **15** 773–844
[118] Herrero M A and Velázquez J J L 1993 *Ann. Inst. H Poincaré, Anal. Non Linéaire* **10** 131–89
[119] Merle F and Zaag H 1998 *Commun. Pure Appl. Math.* **51** 139–196

[120] Galaktionov V A and Vázquez J L 2002 *Discrete Contin. Dyn. Syst.* **8** 399–433
[121] Vazquez J L 2006 *Smoothing and Decay Estimates for Nonlinear Diffusion Equations. Equations of Porous Medium Type* (Oxford: Oxford University Press)
[122] Eggers J, Fontelos M A, Leppinen D and Snoeijer J H 2007 *Phys. Rev. Lett.* **98** 094502
[123] Longuet-Higgins M S, Kerman B R and Lunde K 1991 *J. Fluid Mech.* **230** 365
[124] Oğuz H N and Prosperetti A 1993 *J. Fluid Mech.* **257** 111
[125] Thoroddsen S T, Etoh E G and Takeara K 2007 *Phys. Fluids* **19** 042101
[126] Bergmann R, van der Meer D, Stijnman M, Sandtke M, Prosperetti A and Lohse D 2006 *Phys. Rev. Lett.* **96** 154505
[127] Herrero M A and Velázquez J J L 1996 *J. Math. Biol.* **35** 177–94
[128] Dyachenko S, Newell A C, Pushkarev A and Zakharov V I 1992 *Physica* D **57** 96–160
[129] Perelman G 2001 *Ann. H Poincaré* **2** 605–73
[130] Merle F and Raphaël P 2004 *Invent. Math.* **156** 565–672
[131] Merle F and Raphaël P 2006 *J. Am. Math. Soc.* **19** 37–90
[132] Fibich G, Gavish N and Wang X 2007 *Physica* D **231** 55–86
[133] Fibich G and Gavish N 2008 *Physica* D **237** 2696–730
[134] Bona J L, Dougalis V A, Karakashian O A and McKinney W R 1995 *Philos. Trans. R. Soc. Lond.* A **351** 107–64
[135] Martel Y and Merle F 2002 *Ann. Math.* **155** 235–80
[136] Martel Y and Merle F 2002 *J. Am. Math.* **15** 617–664
[137] Constantin A and Escher J 1998 *Acta Math.* **181** 229–243
[138] Lister J R and Stone H A 1998 *Phys. Fluids* **10** 2758
[139] Plateau J A F 1843 *Acad. Sci. Bruxelles Mem.* **16** 3
[140] Gundlach C 2003 *Phys. Rep.* **376** 339–405
[141] Pumir A, Shraiman B I and Siggia E D 1992 *Phys. Rev.* A **45** R5351
[142] Sornette D 1998 *Phys. Rep.* **297** 239–70
[143] Hirschmann E W and Eardley D M 1997 *Phys. Rev.* D **56** 4696–4705
[144] Aichelburg P C, Bizon P and Tabor Z 2006 *Class. Quantum Grav.* **23** S299–S306
[145] Pumir A and Siggia E D 1992 *Phys. Fluids* A **4** 1472
[146] Pumir A and Siggia E D 1992 *Phys. Rev. Lett.* **68** 1511
[147] E W and Shu C W 1994 *Phys. Fluids* **6** 49
[148] McKay S R, Berker A N and Kirkpatrick S 1982 *Phys. Rev. Lett.* **48** 767
[149] Strogatz S H 1994 *Nonlinear Systems and Chaos* (Boulder, CO: Westview Press)
[150] Lorenz E N 1963 *J. Atmos. Sci.* **20** 130
[151] Almgren R 1996 *Phys. Fluids* **8** 344
[152] Constantin P, Dupont T F, Goldstein R E, Kadanoff L P, Shelley M J and Zhou S 1993 *Phys. Rev.* E **47** 4169
[153] Almgren R, Bertozzi A L and Brenner M P 1996 *Phys. Fluids* **8** 1356
[154] Bertozzi A L, Brenner M P, Dupont T F and Kadanoff L P 1994 *Applied Mathematics Series* vol 100 ed L Sirovich (Springer: New York) p 115
[155] Bizón P, Maison D and Wasserman A 2007 *Nonlinearity* **20** 2061–74
[156] Merle F and Zaag H 2007 *J. Funct. Anal.* **253** 43–121
[157] Merle F and Zaag H 2008 *Commun. Math. Phys.* **282** 55
[158] Merle F and Zaag H 2008 *Preprint* arXiv:0811.4068
[159] Souplet P 2001 *Electron. J. Diff. Eqns* **20** 1–19
[160] Fontelos M A and Velázquez J J L 2000 *Eur. J. Appl. Math.* **11** 29
[161] Caffarelli L, Kohn R and Nirenberg L 1982 *Commun. Pur. Appl. Math.* **35** 771–831
[162] Constantin P and Foias C 1994 *Navier–Stokes Equations* (Chicago, IL: University of Chicago Press)
[163] Smoller J 1989 *Shock Waves and Reaction–Diffusion Equations* (New York: Springer)